The Islamic University–Gaza

Research and Postgraduate Affairs

Faculty of Science

Master of Physics

الجامعـــــــة الإســـلاميـة – غـزة

شئون البحث العلمي والدراسات العليا

كليـــــــــــة العلـــــــــوم

مـاجســـــتير الفـيـــزيـــــاء

Number of Neighbours and Lattice Size Effects in Semi-Directed Barabási-Albert Networks

تأثيرات حجم وعدد المجاورات في الشبكة البلورية على شبكات ألبرت برابيزي الشِّبه مباشرة

Presented By

Areej Mohammed Ata El Bitar

Supervised by

Prof.Dr. Mohammed M. Shabat

A thesis submitted in partial fulfillment
of the requirements for the degree of
Master of Science in Environmental Sciences

May/2016

إقـــــرار

أنا الموقع أدناه مقدم الرسالة التي تحمل العنوان:

Number of Neighbours and Lattice Size Effects in Semi-directed Barabási-Albert Networks

تأثيرات حجم وعدد المجاورات في الشبكة البلورية على شبكات ألبرت برابيزي الشِّبه مباشرة

أقر بأن ما اشتملت عليه هذه الرسالة إنما هو نتاج جهدي الخاص، باستثناء ما تمت الإشارة إليه حيثما ورد، وأن هذه الرسالة ككل أو أي جزء منها لم يقدم من قبل الاخرين لنيل درجة أو لقب علمي أو بحثي لدى أي مؤسسة تعليمية أو بحثية أخرى.

Declaration

I understand the nature of plagiarism, and I am aware of the University's policy on this.

The work provided in this thesis, unless otherwise referenced, is the researcher's own work, and has not been submitted by others elsewhere for any other degree or qualification.

Student's name:	أريج محمد عطا البيطار	اسم الطالب:
Signature:	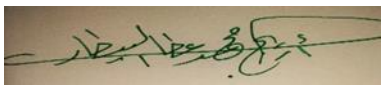	التوقيع:
Date:	4/5/2016	التاريخ:

بسم الله الرحمن الرحيم

الجامعة الإسلامية – غزة
The Islamic University - Gaza
مكتب نائب الرئيس للبحث العلمي والدراسات العليا هاتف داخلي 1150

الرقم Ref ج س غ/35/
التاريخ Date 02/06/2016

نتيجة الحكم على أطروحة ماجستير

بناءً على موافقة شئون البحث العلمي والدراسات العليا بالجامعة الإسلامية بغزة على تشكيل لجنة الحكم على أطروحة الباحثة/ أريج محمد عطا البيطار لنيل درجة الماجستير في كلية العلوم قسم الفيزياء وموضوعها:

(تأثير حجم وعدد المجاورات في الشبكة البلورية على شبكات ألبرت برابيزي الشبه مباشرة)

(Number of Neighbours and Lattice Size Effects in Semi-Direct Barabasi –Albert Network)

وبعد المناقشة العلنية التي تمت اليوم الاربعاء 27 رجب 1437هـ، الموافق 2016/05/04م الساعة الحادية عشرة صباحاً بمبني اللحيدان، اجتمعت لجنة الحكم على الأطروحة والمكونة من:

أ.د. محمد موسى شبات	مشرفاً و رئيساً	.....
أ.د. ناصر اسماعيل فرحات	مناقشاً داخلياً	.....
د. منير أحمد سمور	مناقشاً خارجياً	.....

وبعد المداولة أوصت اللجنة بمنح الباحثة درجة الماجستير في كلية العلوم/ قسم الفيزياء.

واللجنة إذ تمنحها هذه الدرجة فإنها توصيها بتقوى الله ولزوم طاعته وأن تسخر علمها في خدمة دينها ووطنها.

والله ولي التوفيق،،،

نائب الرئيس لشئون البحث العلمي والدراسات العليا

أ.د. عبدالرؤوف علي المناعمة

P.O. Box 108, Rimal, Gaza, Palestine fax: +970 (8) 286 0800 فاكس Tel: +970 (8) 286 0700 ص.ب. 108 الرمال، غزة، فلسطين هاتف
public@iugaza.edu.ps www.iugaza.edu.ps

Abstract

The present work continues the study of two semi-directed BA networks, SDBA1 and SDBA for much larger m than before. In these semi-directed networks, the exponent γ for the power law governing the decay of the number $n(k)$ of nodes having(k)neighbors, $n(k)\sim 1/k^{-\gamma}$, depends continuously on the parameter m, and the behavior for m → ∞ is studied.

The effect of different finite size with constant number of neighbours m and the effect of different number of neighbors with constant lattice size on two versions (SDBA1 and SDBA2) for semi-directed Barabási-Albert networks are evaluated to find out the size effects vary with m.

Keywords: Directed BA Network, Undirected BA Network, Semi-directed BA Network.

Abstract in Arabic

الملخص

إن العمل الحالي يكمل دراسة شبكتين ألبرت برابيزي الشبه مباشرة لm أكبر بكثير من الأول. وفي هذه الشبكات الشبه مباشرة فإن الدليل γ لقانون القوة الذي يحكم تلاشي الرقم$n(k)$ للعقد (k)التي تجاورها.$n(k)\sim k^{-\gamma}$ يعتمد بصفة مستمرة على التدرج m حيث نود معرفة شكله السلوكي عندما تؤول إلى ما لانهاية.

والآن نفحص تأثير الحجم المحدود بأرقام ثابتة لمتجاورات m ولتأثيرات المتجاورات لأرقام مختلفة بحجم شبكة ثابتة على النظامين لشبكات ألبرت برابيزي لمعرفة كيف يؤثر تغيير الحجم على m .

Dedication

To those whom God Almighty recommended to obey them and related his content to their content my dear parents: Mum and Dad who did their best to get me to the highest degree of success. I dedicate this work.

To my reliable brothers Ahmed and Adham and to my sweet twins: my sister Enas and Amani, I also dedicate this work.

I never forget to dedicate this work to everyone has a hand in helping me to finish this work whatever small his help was.

Acknowledgment

I would like to express my deep thanks and innermost gratitude to my supervisor Prof.Dr. Mohammed M. Shabat for his remarkable guidance and unforgettable kindness to me which facilitated my mission.

I would like to thank Prof. Dietrich Stauffer from Germany, and Dr.F.W.S. Lima from Brazil for their help.

I never forget to thank heartily Dr. Muneer A. Sumour and Dr. Mohammed A. Radwan for many valuable suggestions, fruitful discussions and constructive advice during the development of this work, and the referee for useful help with the thesis.

I'd like to thank my teacher Alia Hadidi for her help.

Additionally, my hearty thanks are also extended to everyone that offered a hand to help me whatever small his help was.

Table of Contents

List of Tables

List of Figures

List of Abbreviations

BA	Barabási-Albert Networks
DBA	Directed Barabási-Albert Network
UDBA	Undirected Barabási-Albert Network
SDBA	Semi-Directed Barabási-Albert Network
MCSN	Monte Carlo Step Number

CHAPTER ONE

ISING MODEL

CHAPTER ONE

ISING MODEL

1.1. Introduction

The Ising model is the simplest and most famous spin system model for the study phase transitions. It was introduced in 1925 by Ernst Ising [1] in his Ph.D. thesis. He solved the model completely for one -dimension, and found that no phase transition occurs. He concluded that this should be the case for all dimensions.

We can calculate the energy of a system by using the Hamiltonian

$$\boldsymbol{H = -J \sum_{<ij>} s_i s_j - h \sum_i s_i} \qquad \textbf{(1.1)}$$

Where $s_i = \pm 1,\ i = 1, \dots, N$ (state of spin)

$< ij >$ *sum of all nearest neighboring pair of spin*

J-coupling constant

h- external magnetic field

[1] About professor Ernst Ising (Heise, Heß, Strecker, & Frank, 2010)
- May 10, 1900 – born in Germany
- 1924 – University of Hamburg, published his doctoral thesis on linear chain of magnetic moments of 1 and -1, and never returned to this research
- 1947 – Ising came to USA and became a teacher of physics and mathematics at State Teachers College in Minot, North Dakota
- 1948 – became a physics professor at Bradley University, Illinois
- May 11, 1998 – He passed away.

1.2. Fundamental Concept

1.2.1. Models in Statistical Mechanics

Statistical Thermodynamics provides a connection between the macroscopic properties of materials in thermodynamic equilibrium, and the microscopic behaviour and motions occurring inside the material(Renn, 1997)

In Statistical physics, a toy model is a simplified set of objects and equations relating them so that they can nevertheless be used to understand a mechanism that is also useful in the full, non-simplified theory. Some examples of "toy models" in Statistical Physics might be: The Ising model and the Potts model as a toy model for ferromagnetism.

1.2.2. Partition Function

Partition functions describe the statistical properties of a system in thermodynamic equilibrium. It is a function of temperature and other parameters, such as the volume enclosing a gas. Most of the aggregate thermodynamic variables of the system, such as the total energy, free energy, entropy, and pressure can be expressed in terms of the partition function or its derivatives.

There are actually several different types of partition functions, each corresponding to different types of statistical ensemble (or, equivalently, different types of free energy). The canonical partition function applies to a canonical ensemble, in which the system is allowed to exchange heat with the environment at fixed temperature, volume, and number of particles. The grand canonical partition function applies to a grand canonical ensemble, in which the system can exchange both heat and particles with the environment, at fixed temperature, volume, and chemical potential. Other types of partition functions can be defined for different circumstances.

As a beginning assumption, assume that a thermodynamically large system is in a constant thermal contact with the environment at a temperature *T,* and both the volume of

the system and the number of constituent particles fixed. This kind of system is called a canonical ensemble. Let us label with *s* (s = 1, 2, 3, ...) the *exact* states (microstates) that the system can occupy, and denote the total energy of the system when it is in microstate *s* as E_s.

Generally, these microstates can be regarded as analogous to discrete quantum states of the system. The canonical partition function is defined as:

$$\boldsymbol{Z = \sum_s e^{-\beta E_s}} \quad , \qquad \textbf{(1.2)}$$

Where the symbol Z is the "partition function" and $\boldsymbol{\beta}$ is the "inverse temperature", which is conventionally defined as**:** $\boldsymbol{\beta = \frac{1}{k_B\, T}}$**,** with k_B denoting Boltzmann's Constant. The term $e^{-\beta E_s}$ is known as the Boltzmann factor.

Suppose a system is subdivided into *N* sub-systems with negligible interaction energy. If the partition functions of the sub-systems are $\zeta_1, \zeta_2, \zeta_3, \ldots \ldots \zeta_N$. then the partition function of the entire system is the *product* of the individual partition functions:

$$\boldsymbol{Z = \prod_{j=1}^{N} \zeta_j} \quad . \qquad \textbf{(1.3)}$$

If the sub-systems have the same physical properties, then their partition functions are equal, $\zeta_1 = \zeta_2 = \zeta_3 = \cdots \ldots = \zeta$ in which case $\boldsymbol{Z = \zeta^N}$**.**

However, there is a well-known exception to this rule. If the sub-systems are actually identical particles, in the quantum mechanical sense that they are impossible to distinguish even in principle, the total partition function must be divided by a *N!* (*N* factorial) **("Partition function (statistical mechanics),")**

$$\boldsymbol{Z = \frac{\zeta^N}{N!}}. \qquad \textbf{(1.4)}$$

1.2.3. Curie Temperature

The Curie temperature (T_c), or Curie point, is the temperature at which a ferromagnetic or a ferromagnetic material becomes paramagnetic on heating; the effect is reversible. A magnet will lose its magnetism if heated above the Curie temperature. The term is also used in piezoelectric materials to refer to the temperature at which spontaneous polarization is lost on heating. An analogous temperature, the Néel temperature, is defined for antiferromagnetic materials.

Below the Curie temperature neighboring magnetic spins are aligned parallel within ferromagnetic materials and anti-parallel in ferromagnetic materials. As the temperature is increased towards the Curie point, the alignment within each domain decreases. Above the Curie temperature, the material is paramagnetic so that magnetic moments are in a completely disordered state. ("Curie-point,")

The destruction of magnetization at the Curie temperature is a second-order phase transition and a critical point where the magnetic susceptibility is theoretically infinite.

1.2.4. Magnetic Susceptibility

Magnetic susceptibility is defined as a physical quantity that characterizes the relation between the magnetic moment(magnetization) of a substance and the magnetic field in the substance.

The volume magnetic susceptibility equals to the ratio of magnetization per unit volume of the substance M to the intensity H of the magnetizing field that is

$$\chi = M/H. \qquad (1.5)$$

Magnetic susceptibility is a dimensionless quantity.

Magnetic susceptibility may be positive or negative. Diamagnets, which are magnetized against rather than with the field, have negative magnetic susceptibility.

For paramagnets and ferromagnets the magnetic susceptibility is positive (they are magnetized with the field). The magnetic susceptibility of diamagnets and paramagnets is low and depends very slightly on *H*.

Magnetic susceptibility attains particularly high values in ferromagnets (from several tens to many thousands of units) and is very strongly and intricately dependent on H. Therefore, the differential magnetic susceptibility $\boldsymbol{\chi = \frac{\partial M}{\partial H}}$ is introduced for ferromagnets. For H = 0, the magnetic susceptibility of ferromagnets isnot equal to zero but rather has the value χ. As $\boldsymbol{H}$ increases, the magnetic susceptibility increases, reaches a maximum, and then declines.

Magnetic susceptibility usually depends on the temperature. The magnetic susceptibility of paramagnets decreases with temperature, conforming to Curie's law. In ferromagnetic solids magnetic susceptibility increases with temperature, reaching a sharp near the Curie point θ. The magnetic susceptibility of antiferromagnets increases with temperature up to the Neel temperature and then decreases according to the Curie-Weiss law. (Veselago & Vinokurova, 1988)

1.2.5.Magnetization

The matter is built up out of atoms, and each atom consists of electrons in motion. The currents associated with this motion are termed *atomic currents*. Each atomic current is a tiny closed circuit of atomic dimensions, and may therefore be appropriately described as a magnetic dipole. If the atomic currents of a given atom all flow in the same plane then the atomic dipole moment is directed normal to the plane (in the sense given by the right-hand rule), and its magnitude is the product of the total circulating current and the area of the current loop. If j(r) is the atomic current density at the point $\mathbf{r}$ then the magnetic moment of the atom is

$$\boldsymbol{m = \frac{1}{2} \int r \times j \, d^3 r \ ,} \qquad \textbf{(1.6)}$$

where the integral is over the volume of the atom. If there are N such atoms or molecules per unit volume then the *magnetization* $\mathbf{M}$ (*i.e.*, the magnetic dipole moment per unit volume) is given by $\mathbf{M} = N\mathbf{m}$.

More generally, $\boldsymbol{M}(\boldsymbol{r}) = \sum_i \boldsymbol{N_i} \ < \boldsymbol{m_i} >$ **(1.7)**

where $< m_i >$ is the average magnetic dipole moment of the ith type of molecule in the vicinity of point $\mathbf{r}$, and N_i is the average number of such molecules per unit volume at $\mathbf{r}$.

Consider a general medium which is made up of molecules which are polarizable and possess a net magnetic moment. It is easily demonstrated that any circulation in the magnetization field $M(r)$ gives rise to an effective current density j_m in the medium. In fact,

$$\boldsymbol{j_m} = \nabla \times \boldsymbol{M}\,, \qquad \textbf{(1.8)}$$

where j_m is current density and called the *magnetization current density* (Fitzpatrick, 2006)

1.2.6. Ferromagnetism

Iron, nickel, cobalt and some of the rare earths (gadolinium, dysprosium) exhibit a unique magnetic behavior which is called ferromagnetism because iron (ferrum in Latin) is the most common and most dramatic example. Samarium and neodymium in alloys with cobalt have been used to fabricate very strong rare-earth magnets.

Ferromagnetic materials exhibit a long-range ordering phenomenon at the atomic level which causes the unpaired electron spins to line up parallel with each other in a region called a domain (The domain is a formation of regions of magnetic alignment from electron spins characteristic of ferromagnetic materials). Within the domain, the magnetic field is intense, but in a bulk sample the material will usually be unmagnetized because

many domains will themselves be randomly oriented with respect to one another. Ferromagnetism manifests itself in the fact that a small externally imposed magnetic field, say from a solenoid, can cause the magnetic domains to line up with each other and the material is said to be magnetized. The driving magnetic field will then be increased by a large factor which is usually expressed as a relative permeability for the material. There are many practical applications of ferromagnetic materials, such as the electromagnet.

Ferromagnets will tend to stay magnetized to some extent after being subjected to an external magnetic field. This tendency to "remember their magnetic history" is called hysteresis. The fraction of the saturation magnetization which is retained when the driving field is removed is called the remanence of the material, and is an important factor in permanent magnets.

All ferromagnets have a maximum temperature where the ferromagnetic property disappears as a result of thermal agitation. This temperature is called the Curie temperature. All the other classes of materials have positive susceptibility. Within these classes the magnitude of the susceptibility varies over a very wide range. However, at sufficiently high temperatures the susceptibility decreases with increasing temperature for all materials in these classes.

It was found experimentally that all these materials follow the relationship

$$\chi = \frac{C}{T - T_c} \quad , \tag{1.9}$$

here C and T_c are positive constants independent of temperature and different for each material. (Zhang, Jiang, & Lin, 2014)

1.2.7. Relation Between the Partition Function and The Various Thermodynamic

In order to demonstrate the usefulness of the partition function, let us calculate the thermodynamic value of the total energy. This is simply the expected value, or ensemble

average for the energy, which is the sum of the microstate energies weighted by their probabilities and given as:

$$< E_s > = \sum_s E_s \; P_s = \frac{1}{Z} \sum_s E_s e^{-\beta E_s} = \frac{-1}{Z} \frac{\partial Z\,(\beta, E_1, E_2, \ldots\ldots)}{\partial \beta} = \frac{-\partial \ln Z}{\partial \beta} \quad . \qquad \textbf{(1.10)}$$

or, equivalently: $$< E > = K_B T^2 \frac{\partial \ln Z}{\partial T} \quad . \qquad \textbf{(1.11)}$$

and the variance in the energy (or "energy fluctuation") given as :

$$< (\Delta E)^2 > = < (E - < E >)^2 > = \frac{\partial^2 \ln Z}{\partial \beta^2} \quad . \qquad \textbf{(1.12)}$$

While the heat capacity calculated by:

$$C_v = \frac{\partial < E >}{\partial T} = \frac{1}{K_B T^2} < (\Delta E)^2 > , \qquad \textbf{(1.13)}$$

And The entropy given as :

$$S \equiv \frac{\partial (K_B T \ln Z)}{\partial T} = \frac{-\partial A}{\partial T} \quad , \qquad \textbf{(1.14)}$$

where *A* is the Helmholtz free energy defined as $A = U - TS$, where $U = \langle E \rangle$ is the total energy and *S* is the entropy, so that $A = < E > - TS = - (K_B T \ln Z)$. **(1.15)**

("Partition function (statistical mechanics),")

1.2.8. Arrhenius Law:

Arrhenius equation in chemistry equation is named after the owner of the world's chemist Svante Arrhenius, which describe the process of time chemical reactions (chemical kinetics), Arrhenius' equation gives the dependence of the rate constant K of a chemical reaction on the absolute temperature T (in kelvins), $K = A \exp(-E_a / RT)$, where A is the pre-exponential factor , E_a is the activation energy ,R and is the universal gas constant (Arrhenius, 1889),(Choudhury, Malhotra, Bhattacharjee, & Prasad, 2014),

1.3. Solving of Ising Model

The Ising model was dissolved form in several stages as follows:

- invented by W. Lenz and his student E. Ising (1920)
- **1D**: solved analytically by Ising (1925): no phase transition in 1D and he concluded incorrectly that in higher dimension also no phase transition occurs.
- **2D** square lattice: solved by L. Onsager (1944), exhibits phase transition also in higher dimensions phase transition can be modeled
- Istrail showed that computation of the free energy of an arbitrary subgraph based on Ising model will not be approximated computationally intractable (not solvable) by any method for the case **3-** dimension and higher. **(Heise et al., 2010)**

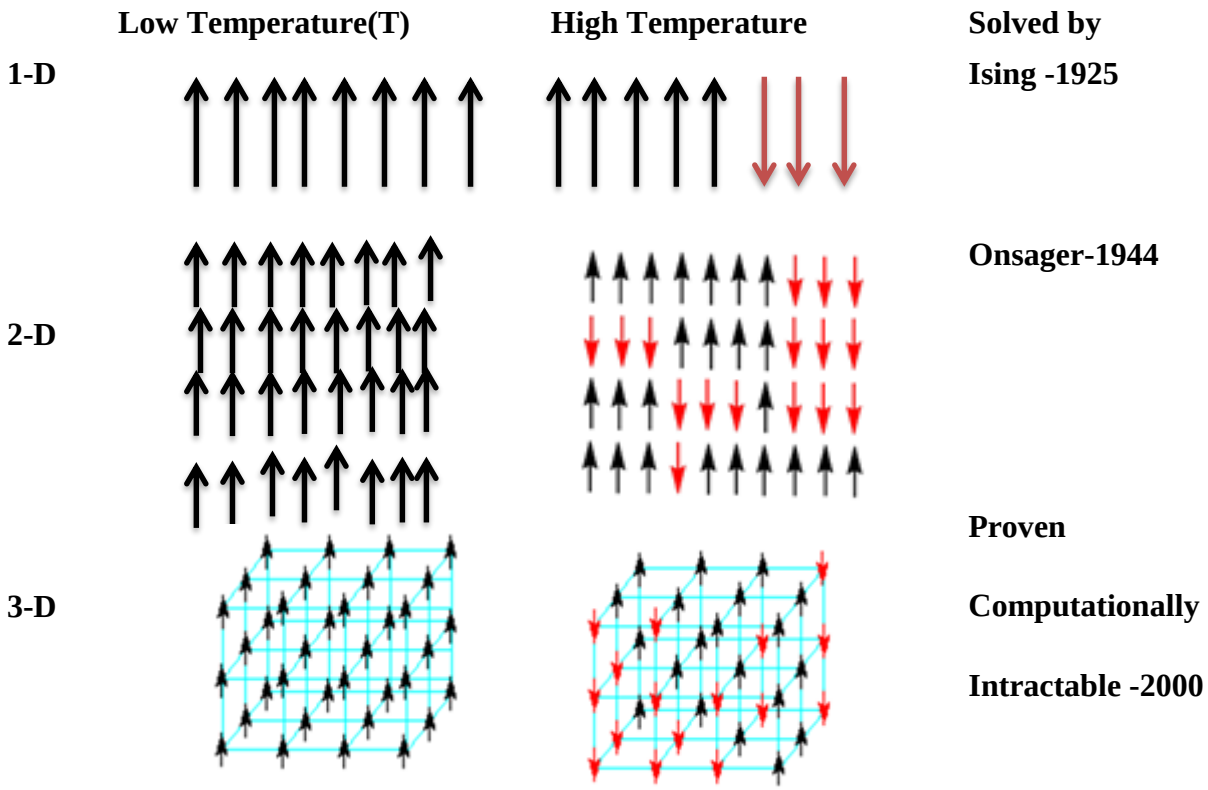

As temperature(T) increases, spin (s) deviate more and more from the common direction, thus increasing the amplitude of spin waves reducing the net magnetization (Peierls, 1936)

1.4. Ising Model Basics

The Ising model has some basic rules, including: **(Iordache, 2000)**

a- A simple, classical model of a magnetic material.

b- A Lattice (usually regular): several points in a set dimension, either 1-D, 2-D,3-D, etc. with a magnet or classical 'spin' at each spin has one of two states (+/-) or directions (up/down). down: $\boldsymbol{S_i} \in \{+\mathbf{1}, -\mathbf{1}\}$ (in Quantum Mechanics Would be $\boldsymbol{S_i} \in \{+\mathbf{1/2}, -\mathbf{1/2}\}$). Each line between points is called a **bond**. If there is a bond connecting two points, they are referred to as nearest neighbours.

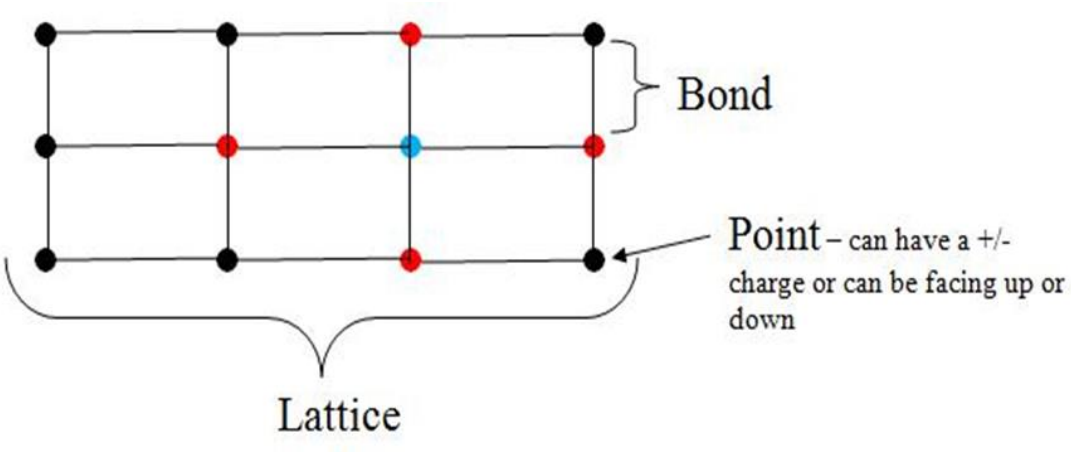

c- The 'Spins' Interact with each other via a coupling of strength ***J*** and to an external applied magnetic field ***h***.

d- The total energy of the 'spins' is the **Hamiltonian**:

$$\boldsymbol{H = -J \sum_{<ij>} s_i s_j - h \sum_i s_i} \quad , \qquad \textbf{(1.17)}$$

Where $s_i = \pm 1,\ i = 1, \ldots, N$ (state of spin)

h- external magnetic field , *J-coupling constant*

If $\boldsymbol{J}$**>0**, we have a **ferromagnetic**. Energy is lowest if all $\boldsymbol{s_i}$ are the same favored.

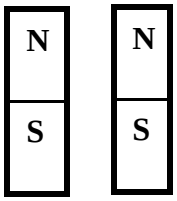

If **J<0**, we have an **antiferromagnetic**. Energy is lowest if neighbouring s_i are opposite favored.

S	**N**
N	**S**

e- Introducing the inverse temperature parameter $\beta=\frac{1}{k_B T}$,

where $k_B = 1.380658\, x\, 10^{-23}\, {}^{J}/_{K}$, *is the Boltzmann constant*

1.5. Ising Model –Statistical Thermodynamics

The Ising microscopical systems model as it is in statistical Thermodynamics , so it is based on the principles of statistical dynamics as follows :**(Huang, 2009)**

a- The probability for the system to in the microstate v defined as:

$$P_v = \frac{1}{Z} exp(-\beta E_v) , \qquad \textbf{(1.18)}$$

where $E_v = -J \sum_{<ij>} s_i s_j$,

For $\beta << \beta_{critical}$ (*i.e.* $T >> T_{critical}$) spins are essentially random (. *i.e.* the probability of all configurations is essentially equal . $\lim_{\beta \to 0} P_v = \frac{1}{Z}$. **(1.19)**

But if $\beta > \beta_{critical}$ (*i.e.* $T < T_{critical}$), then for $J>0$, configurations with almost all spins aligned are much more probable. Where $T_{critical}$ is the Neél or Curie Temperature. For J=1, $\beta_{critical}$~0.44 or $T_{critical}$~1.6.

b- The partition function is defined as:

$$\mathbf{Z(\beta, h)} = \sum_v \exp(-\beta E_v) . \qquad \textbf{(1.20)}$$

c- The Magnetization:

If no magnetic field term in h, h=0, then the magnetism is defined as:

$M_v = \sum_{i=1}^{N} s_i$ or $M_v = -\frac{\partial f}{\partial h}$,where ($f = -k_\beta T \ln(z)$) is the free energy, and if h≠0, then The magnetization is a function of β and h.

d- The Mean Magnetization is given as:

$$\boldsymbol{M \equiv < M_v > = \frac{1}{Z} \sum_{v} M_v \exp(-\beta E_v)} \qquad (\mathbf{1.21})$$

e- The Mean Energy is given as :

$$\boldsymbol{U \equiv < E_v > = \frac{1}{Z} \sum_{v} E_v \exp(-\beta E_v)} \qquad \mathbf{(1.23)}$$

In **Figure (1.1)**

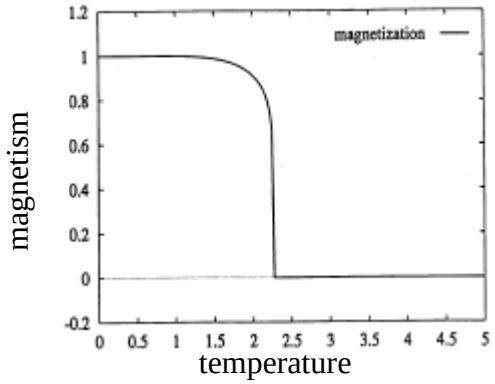

Figure (1.1): show Magnetization in zero external field, as function of temperature. **(Huang, 2009)**

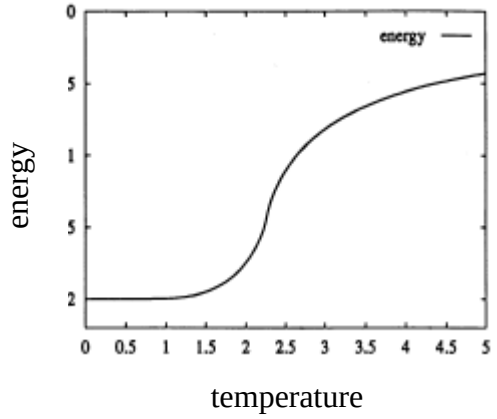

Figure (1.2): shows the relationship between energy versus temperature ($\boldsymbol{E_v} \propto \boldsymbol{T}$)

(Huang, 2009)

1.6. Applications for Ising Model

Ising model has several applications in different fields including, the following :**(Heise et al., 2010)**

a- Magnetism:

*In 19th century: two theories: Ampere postulated that the permanent magnets due to permanent internal atomic currents versus. The theory of permanent magnetic moment as:

- Electron spin discovered to describe magnetism
- Ising model: investigate if electrons could be made to spin in same direction by simple local forces

  the magnetism defined : $\boldsymbol{M_v} = \sum_{i=1}^{N} \boldsymbol{s_i}$ or $\boldsymbol{M_v} = -\frac{\partial f}{\partial h}$

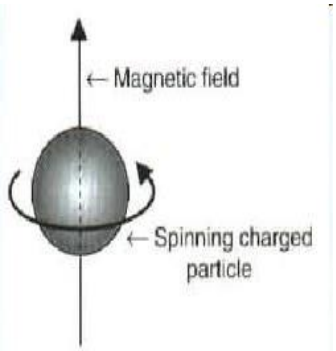

Figure (1.3): As electrons orbit around the nucleus, they create a magnetic field.

b- Lattice gas:

- Interpret Ising model as a statistical model where B =[0,1],[unoccupied ,occupied] → B = (σ + 1)/2 → σ = [-1,1]

$$\boldsymbol{H = -J \sum_{<ij>} B_i B_j} \qquad \textbf{(1.26)}$$

The density of atoms can be controlled by chem pot μ

$$\boldsymbol{H = -J \sum_{<ij>} B_i B_j - \sum_i u\, B_i} \qquad \textbf{(1.27)}$$

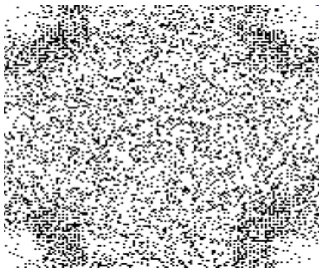

Figure (1.4): density of atoms

c- Biologic – neurons in brain:

Ising model has been applied in the biology of the human body as in states: firing, not firing .To reproduce average **firing rate** for each neuron includes activity of each neuron (statistically independent) $\boldsymbol{H = -\sum_i u\, S_i}$ **(1.28)**

To allow for pair interactions when a neuron tends to fire along with another

$$\boldsymbol{H = -\frac{1}{2}\sum_{<ij>} J\, s_i s_j - \sum_i h\, s_i} \qquad \textbf{(1.29)}$$

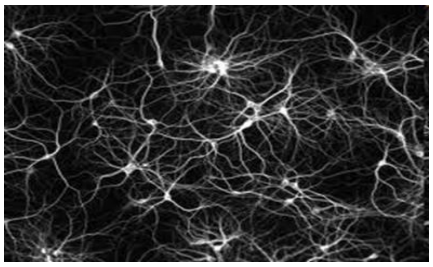

Figure (1.5): for pair interactions when a neuron tends to fire along with another

J – NN interaction of firing rate. h – self-firing rate

This energy function only introduces probability biases for a spin having a value and for a pair of spins having the same value

CHAPTER TWO

BARABÁSI ALBERT NETWORK

CHAPTER TWO

BARABÁSI ALBERT NETWORK

2.1. Introduction

The system feature in natural systems is always a source of inspiration and beauty as related to physical and biological sciences where arranging crystals is the most important foundation of many developments in contemporary physics and complex systems in nature **(Barabási, Albert, & Jeong, 2000)**. In fact, some of the systems around us give us a complex topology that appears somewhat random and unexpected, particularly the complex systems of networks consisting of vertices representing elements of the system and edges that represent the interactions between them. For example, genes in which the system 's proteins are the vertices while the chemical interactions between proteins are edges. Similar is the formation of an extensive network in the nervous system, and the which are vertices nerve cells, while the edges are neurons. But equally complex networks occur in social science, where vertices are individuals or organizations and the edges characterize the social interactions between them (Wasserman & Faust, 1994), in the business world, where vertices are companies and edges represent diverse trade relationships, or describe the world-wide web (www) whose vertices are HTML documents connected by links pointing from one page to another (Barabási et al., 2000),(Kaltenbrunner et al., 2007) . The most important step is to understand the general characteristics of network development concerning the recent discovery of a surprising degree of self-organization characterizing the large scale properties of complex networks. Exploring several large databases describing the topology of large networks, that span as diverse fields as the www or the citation patterns in science, recently proved that independence of the nature of the system and the identity of its components, the probability P(k) that a vertex in the network is connected to k other vertices decays as a power-law, following $P(k) \sim k^{-\gamma}$. These results offered the first evidence that large

networks self-organize into a scale-free state, a feature unexpected by all existing random network models.(Newman, Barabasi, & Watts, 2006)

This chapter, explains the history of the concept of the Preferential attachment to reach Barabási- Albert networks, and will also discusses the network and degrees of dynamics and degrees of distributions through continuum theory, at the end of the chapter I refer to Albert Barabási networks applications

2.2 A Brief History

Preferential attachment has emerged repeatedly in mathematics and social sciences. Consequently, today we can encounter it under different names in the scientific literature, as fellow:

• It made its first appearance in 1923 in the celebrated urn model of the Hungarian mathematician Gyorgy Polya (1887-1985) (Albert & Barabási, 2002) , proposed to explain the nature of certain distributions. Hence, in mathematics preferential attachment is often called a Polya process.

• George Udmy Yule (1871-1951) in 1925 used preferential attachment to explain the power-law distribution of the number of species per genus of flowering plants(Yule, 1925). Hence, in statistics preferential attachment is often called a Yule process.

• Rober Gibrat (1904-1980) in 1931 proposed that the size and the growth rate of a firm are independent. Hence, larger firms grow faster(Gibrat & Les Inégalites Économiques, 1931). Called proportional growth, this is a form of preferential attachment.

• George Kinsley Zipf (1902-1950) in 1941 used preferential attachment to explain the fat tailed distribution of wealth in the society (Zipf, 1949).

• Modern analytical treatments of preferential attachment use of the master equation approach are pioneered by the economist Herbert Alexander Simon (1916-2001). Simon

used preferential attachment in 1955 to explain the fattailed nature of the distributions describing city sizes, word frequencies in a text, or the number of papers published by scientists(Simon, 1960) .

• Building on Simon's work, Derek de Solla Price (1922-1983) used preferential attachment to explain the citation statistics of scientific publications, referring to it as cumulative advantage (Price, 1976) .

• In sociology preferential attachment is often called the Matthew effect, named by Robert Merton (1910-2003) (Merton, 1968) after a passage in the Gospel of Matthew: "For everyone who has will be given more, and he will have an abundance. Whoever does not have, even what he has will be taken from him."

• The term preferential attachment was introduced in the 1999 paper by Barabási[2] and Albert (Barabási & Albert, 1999) to explain the ubiquity of power laws in networks. **(Barabási & Frangos, 2014)**

[2] About professor Barabási Albert:(Barabási et al., 2000)

Albert-László Barabási (born March 30, 1967) is a Romanian-born Hungarian-American physicist, best known for his work in the research of network theory. He is the former Emil T. Hofmann professor at the University of Notre Dame and current Distinguished Professor and Director of Northeastern University's Center for Complex Network Research (CCNR) associate member of the Center of Cancer Systems Biology (CCSB) at the Dana–Farber Cancer Institute, Harvard University, and professor at the Center for Network Science at Central European University.
He introduced in 1999 the concept of scale-free networks and proposed the Barabási–Albert model to explain their widespread emergence in natural, technological and social systems, from the cellular telephone to the World Wide Web or online communities.

2.3. The Barabási-Albert Model

The recognition that growth and preferential attachment coexist in real networks which has inspired a minimal model called **the Barabási-Albert model**, which can generate scale-free networks (Barabási & Frangos, 2014) . Also known as the BA model or the scale-free model, it is defined as follows:

Starting with m_o nodes, the links which are chosen arbitrarily, as long as each node has at least one link. The network develops the following two steps (Figure 2.1):

(A) **Growth**

At each time step added a new node with ***m*** ($\leq m_o$) links that connect the new node to ***m*** nodes already in the network.

(B) **Preferential attachment**

The probability $P(k)$that a link of the new node connects to node i depends on the degree k_i as

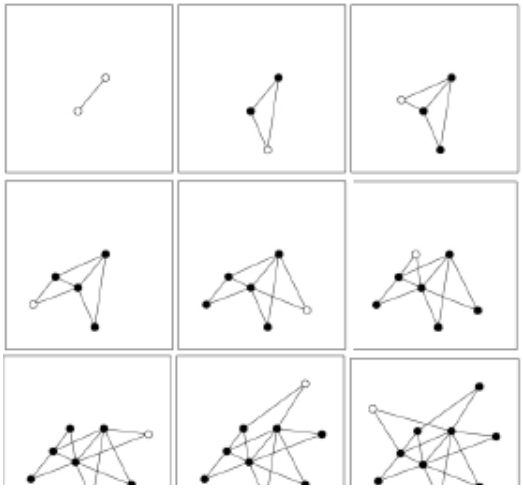

Figure2. 1 show generating the BA networks

$$\boldsymbol{P(k_i) = \frac{k_i}{\sum_i k_i}} \qquad \textbf{(2.1)}$$

Preferential attachment is a probabilistic mechanism: A new node is free to connect to any node in the network, whether it is a hub or has a single link. Equation (1) implies, however, that if a new node has a choice between a degree-two and a degree-four node, it is twice as likely that it connects to the degree-four node. After t time steps the Barabási-Albert model generates a network with N=t+m_o nodes and $N_o + mt$ links. WhereN_o is initial number of links between the initial m_o nodes. As Figure (2.2) shows the obtained network having a power-law degree distribution with degree exponent γ=3. **(Barabási & Frangos, 2014)**

As Figure (2.1), while most nodes in the network have only a few links, a few gradually turn into hubs. These hubs* are the result of a rich-gets-richer phenomenon: Due to preferential attachment new nodes are more likely to connect to the more connected nodes than to the smaller nodes. Hence, the larger nodes will acquire links at the expense of the smaller nodes, eventually becoming hubs.

In brief, the Barabási-Albert model indicates that two simple mechanisms, *growth* and *preferential attachment* which are responsible for the emergence of scale-free networks. The origin of the power law and the associated hubs are a *rich-gets-richer phenomenon* induced by the coexistence of these two ingredients.

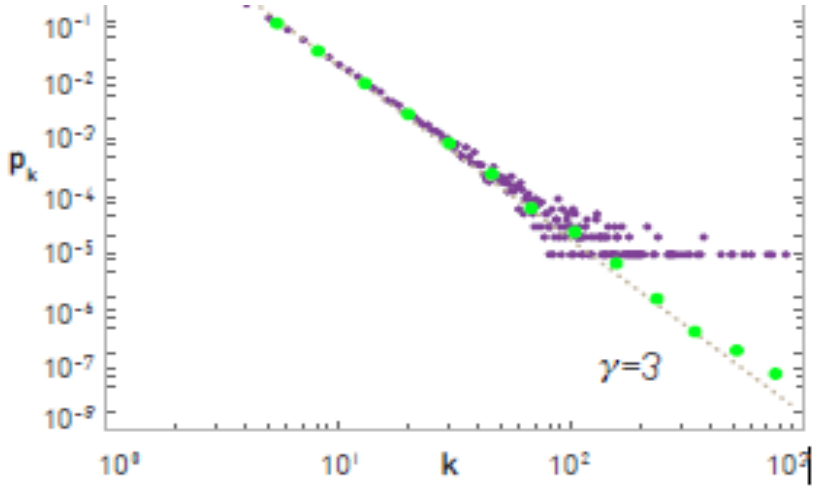

Figure (2.2): The degree distribution of a network generated by the Barabási-Albert model. The figure shows $\boldsymbol{P}(\boldsymbol{k})$ for a single network of size N=100,000 and m=3. It shows both the linearly- binned (purple) and the log-binned version (green) of $\boldsymbol{P}(\boldsymbol{k})$. The straight line is added to guide the eye and has slope γ=3, corresponding to the networks predicted degree exponent

* hubs: The popular nodes

2.4. Degree Dynamics

To find out the properties of the scale-free networks what is known (Barabási-Albert model), we must focus on the temporal evolution her. Starting by exploring the time-dependent degree of a single node(Jeong, Tombor, Albert, Oltvai, & Barabási, 2000).

In the model an existing node can increase its degree each time and a *new* node enters the network. This new node will link to *m* of the *N*(*t*) nodes already present in the system. The probability that one of these links connects to node *i* is given by Equation (2.1). **(Albert & Barabási, 2002)**

Let us approximate the degree $\boldsymbol{k_i}$ with a continuous real variable, representing its expectation value over many realizations of the growth process, that at each time step $(t \rightarrow t+1)$ one node with *m* links is added.

The Time rate at which an existing node *i* acquires links as a result of new nodes connecting to it, is

$$\frac{\partial K_i}{\partial t} \propto P(k_i) = m \frac{K_i}{\sum_j K_j}, \quad \textbf{(2.2)}$$

The coefficient *m* describes that each new node arrives with *m* links.

Hence, node *i* has *m* chances to be chosen. The sum in the denominator of Equation (2.2) goes over all nodes in the network except the newly added node, thus

$$\sum_{j=1}^{N-1} K_j = 2mt - m \quad \textbf{(2.3)}$$

Therefore, Equation (2.2) becomes $\frac{\partial K_i}{\partial t} = \frac{K_i}{2t-1}$

For large t the (-1) term can be neglected in the denominator, obtaining

$$\frac{dK_i}{K_i} = \frac{1}{2}\left(\frac{1}{t}\right)dt \quad \textbf{(2.4)}$$

By integrating Equation (2.4) and using the fact that $\boldsymbol{K_i\ (t_i\ ) = m}$, meaning that node *i joins* the network at time t_i with *m* links, we obtain

$$\boldsymbol{K_i\ (t) = m\ (\frac{t}{t_i})^{\beta}} \qquad \textbf{(2.5)}$$

We call β the *dynamical exponent* and has the value β = $\frac{1}{2}$

2.5. Degree Distribution

A number of analytical tools are available to calculate the degree distribution of the Barabási-Albert network. **(Barabási & Frangos, 2014)** The simplest is the *continuum theory*, where it predicts the degree distribution $\boldsymbol{P(K) = 2\ m^{\frac{1}{\beta}}\ k^{-\gamma}}$, **(2.6)**

with $\boldsymbol{\gamma = \frac{1}{\beta}\ + 1 = 3}$.

2.5.1. Continuum Theory

To calculate the degree distribution of the Barabási-Albert model in the continuum approximation, firstly calculate the number of nodes with a degree smaller than *k,* i.e. $K_i\ (t) < k$. Using Equation (2.5) we write

$\boldsymbol{t_i\ < t\ (\frac{m}{k})^{\frac{1}{\beta}}}$, In the model one node is added at equal time step Therefore the number of nodes with a degree smaller than *k* is $\boldsymbol{t\ (\frac{m}{k})^{\frac{1}{\beta}}}$.

Altogether there are $N=m_o+t$ nodes, which becomes $N \approx t$ in the large *t* limit. Therefore, the probability that a randomly chosen node has degree *k* or smaller, which is the cumulative degree distribution, follows $\boldsymbol{p(k) = 1 - (\frac{m}{k})^{\frac{1}{\beta}}}$, **(2.7)**

by taking the derivative of Equation (2.7), we obtain the degree distribution

$$\boldsymbol{p_k = \frac{\partial p(k)}{\partial k} = \frac{1}{\beta} \frac{m^{\frac{1}{\beta}}}{k^{\frac{1}{\beta}+1}} = 2m^2k^{-3}}\ , \qquad \textbf{(2.8)}$$

which is Equation (2.6) **(Barabási & Frangos, 2014).**

2.6. Barabási-Albert Networks Types

As has already been dealt with the Barabási-Albert model. we will look at the most important of types as follows:

The first type: Price model created a *directed* graph with variable numbers of edges added to each node. It gives the degree distribution $P(k) \sim k^{-\gamma}$. **(Hong, Damrauer, Carroll, & Berry, 1993)** .Direct Barabási-Albert networks (DBA)/ Price model keeps the growing character of the network without preferential attachement. Starting with a small number of nodes (m_o)t, at every time step, we add a new node to m(<m_o), edges. We assume that the new node is connected with equal probability to the nodes already existing in the system, i.e.

$\boldsymbol{P(k_i) = \frac{1}{(m_o+t-1)i}}$ independent of k_i .**(Albert & Barabási, 2002)**

The Second type : Thirty years after, in 1999, Barabási and Albert came with their model: *undirected*, constant number of edges, always gives $P(k) \sim k^{-\gamma}$ **(Huang, 2009)**.

Undirect Barabási-Albert Networks (UDBA) : starts with N nodes. Usually all N nodes are connected to each other add to the List ″This Kert'esz" At each time step a node is selected randomly and connected with probability $\boldsymbol{P(k_i) = \frac{k_i}{\sum_i k_i}}$ to a node i in the system.(Albert & Barabási, 2002).

The Third type : Semi-direct Barabási-Albert Networks(SDBA)

If one adds to the List the m old nodes, plus only once and not m times the new node, one gets a **semi-directed network (SDBA**). Now we check the number of neighbours on two versions (SDBA1 and SDBA2) for semidirected Barabási-Albert networks.

SDBA2 does not give the proper power laws for large m but it does so for small m, whereas SDBA1 gives the proper power laws for large and small m. The resulting exponents vary with m. (M. Sumour, Lima, Radwan, & Shabat, Al-Aqsa University Journal (Natural Sciences Series),Vol.19, No.1, Pages 50-62,Jan.2015 ISSN 2070-3155)

The first version SDBA1 builds the network as follow : new node **n** selects **m** sites **j** which **n** will all influence, while **n** will be influenced only by the first selected j. Our second version SDBA2 inverts the direction of the spin interaction : The new node n selects m sites j which will all influence n, while n will influence only the first selected j. (M. Sumour et al.)

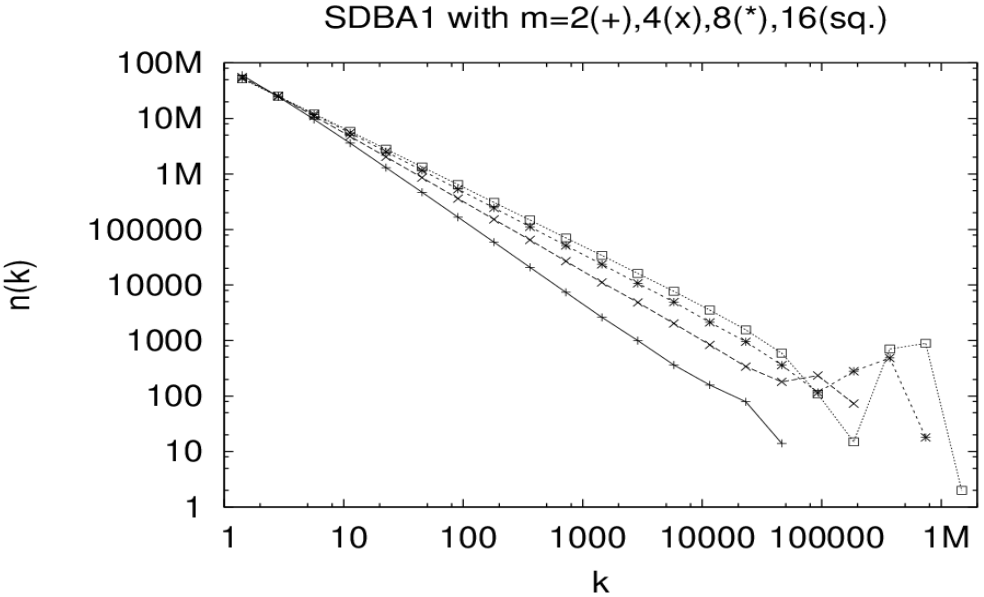

Figure (2.3): Number of nodes n(k) versus k with different m=2 to 16 and N=1,000,000for SDBA1. (M. Sumour et al.)

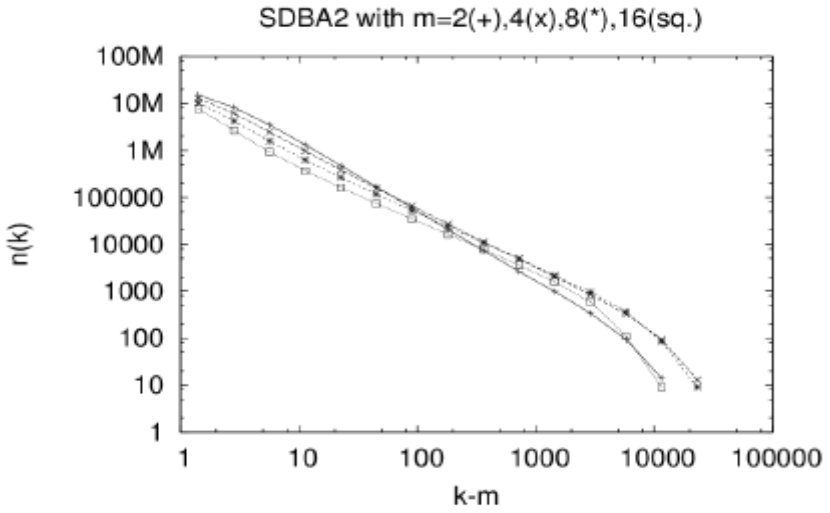

Figure (2.4): Number of nodes n(k) versus k-m with different m=2 to16 and N=1,000,000 for SDBA2(M. Sumour et al.)

As shown in figures (2.3) and (2.4), we can determine a nice slopes in log-log plots of n(k) versus k for SDBA1, while for large m, bad power law is seen for SDBA2**.**

2.7. Applications for Barabási-Albert Model:

Indeed, behind each complex system, there is an intricate network that encodes the interactions between the system's components;

a- The network describes the interactions between genes, proteins, and metabolites integrates the processes behind living cells, and the wiring diagram capturing the connections between neural cells holds the key to our understanding of brain functions.

b- The sum of all professional, friendship, and family ties is the fabric of the society.

c- The network describing which communication devices interact with each other, capturing internet connections or wireless links, is the heart of the model.

d- The power grid, a network of generators and transmission lines, supply energy virtually to all modern technology.

e- Trade networks maintain our ability to exchange goods and services, being responsible for the material prosperity that an increasing fraction of the world has been enjoyed since WWII (World WarII) They also play a key role in the spread of financial and economic crises.

f- Networks are at the heart of some of the most revolutionary technologies of the 21st century, empowering everything from Google to Facebook, CISCO, and Twitter. At the end, networks permeate science, technology, and nature to a much higher degree than may be evident upon a casual inspection. Consequently, it is increasingly clear that we will never understand complex systems unless we gain a deep understanding of the networks behind them. **(Lander et al., 2001)**

g- Epidemics: From forecasting to halting deadly viruses.

While the H1N1 pandemic was not as devastating as it was feared at the beginning of the outbreak in 2009, it gained a special role in the history of epidemics: it was the first pandemic whose course and time evolution were accurately predicted months before the pandemic reached its peak. This was possible thanks to fundamental advances in understanding the role of networks in the spread of viruses. Indeed, before 2000 epidemic modeling was dominated by compartment models, assuming that everyone can infect everyone else, one word: the same socio-physical compartment. The emergence of a network-based framework has fundamentally changed this, offering a new level of predictability in epidemic phenomena. **(Lander et al., 2001)**

h- Brain Research: Mapping neural network.

The human brain, consisting of hundreds of billions of interlinked neurons, is one of the least understood networks from the perspective of network science. The reason is simple: we lack maps telling us which neurons link to each other. The only fully mapped neural map available for research is that of the C. Elegans worm, with only 300 neurons. Should detailed maps of mammalian brains become available, brain research could become the

most prolific application area of network science. Driven by the potential impact of such maps, in 2010 the National Institutes of Health have initiated the Connectome project, aimed at developing the technologies that could provide an accurate neuron-level map of mammalian brains. **(Venter et al., 2001)**

i- Health: From drug design to metabolic engineering.

The human genome project, completed in 2001, offered the first comprehensive list of the whole human genome. Yet, to fully understand how our cells function, and the origin of disease, we need accurate maps that tell us how these genes and other cellular components interact with each other. Most cellular processes, from the processing of food by our cells to sensing changes in the environment, rely on molecular networks. **(Venter et al., 2001)**

CHAPTER THREE

POTTS MODEL

3.1. Introduction

3.2. The Potts Model Hamiltonian

3.3. The Potts Model Partition Function

3.4. Applications for Potts Model

CHAPTER THREE

POTTS MODEL

3.1. Introduction

The Potts model studies long term behaviour of complex systems. The model is able to investigate how the internal elements of the system react with one another based on certain characteristics that each element has. As these reactions take place macroscopic properties of the system will evolve. The Potts model is a very important model, and has wide applications in various fields such as biology, sociology, physics, and chemistry. (Beaudin, Ellis-Monaghan, Pangborn, & Shrock, 2010)

The Potts model's origins date back to the mid-1900s. Two mathematicians, Julius Ashkin and Edward Teller (Ashkin & Teller, 1943), were among the first to experiment with a mathematical model which simulated behavior of various elements within a system.

Intrigued by the model, Cyril Domb suggested the topic to his Ph.D. student, Renfrey B. Potts(Potts, 1952) .With the foundation set by Ashkin and Teller, Potts was able to construct a very useful model. In 1952 he published his doctoral thesis in which he described this particular model (Potts, 1952) The form which the model takes today is known as the q –state Potts model.

This chapter explains the Potts model Hamiltonian, and also discusses the Potts Model Partition Function. At the end of the chapter I talk about Potts Model applications.

3.2. The Potts Model Hamiltonian

The Potts model is a very important mathematical model that studied behaviour in complex system. The model studies the microscopic internal elements and relates their interactions to the macroscopic result which can be observed over time.

Every vertex of the graph will be assigned a spin. The combination of a spin and an adjacency determines which elements will interact with one another.

In general, the spins take the value as 1...*q* where. When $q = 2$ the Potts model is known as the Ising model. The interaction of different spins with each other depend on their position on the graph and their specific values. They measure the total energy of the system**(Chang & Shrock, 2001)** .

The function which measures the total energy of a complex system is the **Hamiltonian**. The Hamiltonian measures the energy of a particular state of a graph by assigning a value to every edge within the complex system . This value depends on the application. In the propriety of the Potts model there are two dominant definitions for the Hamiltonian of a system. The next section shows that these definitions yield equivalent forms of the Potts model partition function. Both definitions use the same notation, *J* is the interaction energy between adjacent elements of the system, and s_i is the spin value assigned to vertex *i* in the state ω. and using the *Kronecher's delta function*,

$$\delta_{s_i, s_j} = \begin{cases} 1 & if\ \sigma_i = \sigma_j \\ 0 & if\ \sigma_i \neq \sigma_j \end{cases} \qquad (3.1)$$

Definition(1) : The first Hamiltonian**(Chang & Shrock, 2001)** is given by,

$$H(\omega) = -J \sum_{<ij>} \delta_{s_i, s_j} \quad , \qquad (3.2)$$

where ω is a state of a graph *G*.

Definition(2): The other definition **(Welsh & Merino, 2000)** for the Hamiltonian is,

$$\boldsymbol{H(\omega) = J \sum_{<ij>}(1 - \delta_{s_i, s_j})} \quad , \tag{3.3}$$

Using **Definition (1):** (Kurinsky, 2015)

$$\boldsymbol{H = -J \sum_{<ij>} \delta_{s_i, s_j} + \sum_i -h \sigma_i} \tag{3.4}$$

where σ_i is a complex vector spaced rotationally equidistant in the complex plane:

$$\boldsymbol{\sigma_i = \exp(\frac{i2\pi s_i}{q})} \tag{3.5}$$

where s_i = 1, 2……., q

The Hamiltonian for the Potts model was given in equation (3.4), where it was stated to be a generalization of Ising Hamiltonian with a small caveat, which needs to be noted before discussing critical properties further. Note that the Ising system has spins s_i = ±1, which can parameterize as $\boldsymbol{\sigma_1}$=1 and $\boldsymbol{\sigma_2}$=2 given that in a q = 2 system, equation (3.5) gives $\boldsymbol{\sigma_1}$ =- 1 and $\boldsymbol{\sigma_2}$= 1.

In addition, we can parameterize their product in the Hamiltonian from the introduction as: $\boldsymbol{s_i s_j = (2\delta_{s_i, s_j} - 1)}$. **(3.6)**

which gives the relation:

$\boldsymbol{Hamiltonian_{Ising} = Hamiltonian_{Potts}}$ at q =2

$$\boldsymbol{H = -J \sum_{<ij>} s_i s_j - h \sum_i \sigma_i = -J \sum_{<ij>} \delta_{s_i, s_j} + \sum_i -h \sigma_i}$$

$$\boldsymbol{= -J \sum_{<ij>}(2\delta_{s_i, s_j} - 1) - h \sum_i \sigma_i = -J \sum_{<ij>} \delta_{s_i, s_j} + \sum_i -h \sigma_i} \tag{3.7}$$

which immediately gives the relation

$$\boldsymbol{J_{Potts}} = 2\,\boldsymbol{J_{Ising}} \qquad \text{or} \qquad \boldsymbol{T_{Ising}} = \frac{1}{2}\,\boldsymbol{T_{Potts}} \ . \tag{3.8}$$

The order parameter defined which describes the average spin state in the system, as the vector mean of all individual spins:

$$\boldsymbol{m} = <\boldsymbol{s}> = \frac{\boldsymbol{1}}{\boldsymbol{N}} \left| \sum_{\boldsymbol{i=1}}^{\boldsymbol{N}} \boldsymbol{exp}\left(\frac{\boldsymbol{i2\pi s_i}}{\boldsymbol{q}}\right) \right| \ , \tag{3.9}$$

such that completely correlated states will evaluate to 1 and uncorrelated states to 0; the phase factors from the uncorrelated states will be cancelled. In addition, the correlation between spins $\boldsymbol{s_i}\,\boldsymbol{s_j}$ according to the coupling in the Hamiltonian can be written as:

$$< \boldsymbol{s_i}\,\boldsymbol{s_j} > = \frac{\boldsymbol{q}}{\boldsymbol{q-1}} \frac{\boldsymbol{1}}{\boldsymbol{N_p}} \sum_{\boldsymbol{s_i}\,\boldsymbol{s_j}}^{\boldsymbol{N_p}} \left(\boldsymbol{\delta}(\ \boldsymbol{s_i} - \boldsymbol{s_j}) - \frac{\boldsymbol{1}}{\boldsymbol{q}} \right) \quad , \tag{3.10}$$

This follows as the simple sum of weighted probabilities. In a completely uncorrelated system, the probability of two spins having the same value is $\frac{\boldsymbol{1}}{\boldsymbol{q}}$, and the correlation will be zero, and in a completely correlated system the expectation of the delta function will be 1, and the value in the sum will evaluate to N (q-1)/ q, giving the correlation a value of 1. **(Kurinsky, 2015**)

3.3. The Potts Model Partition Function

The partition function of the q-state Potts model is defined by

$$\boldsymbol{Z} = \sum \mathbf{exp}(-\boldsymbol{\beta H}) \quad , \tag{3.11}$$

The *Potts model probability function* is the function which calculates the probability of finding the lattice in a particular state. This probability function depends on the Boltzmann distribution from statistical mechanics (for a system following the Boltzmann distribution

laws the number of particles in a given energy state are exponentially distributed.)

$$\boldsymbol{P} = \frac{1}{Z}\exp(-\beta H)$$

so the probability of occurrence of a state now depends solely on the temperature of the system. Table (3.1) shows how the probability changes regarding the system's temperature (Tran, 2013)

Table (3.1) shows how the probability changes regarding the system's temperature**.**

Temperature	Probability
0.01	0.5 or 50%
1.00	0.27 or 27%
2.00	0.149 or 14.9%
10	0.076 or 7.6%
100	0.0637 or approx. 1/16

As can be seen the probability of having all particles with the same state is the highest at low temperature, when the ferromagnetic particles prefer same direction alignment, and the free energy in the system is not enough for most of the particles to change state. Higher temperature brings more free energy to the system, and when the temperature is high enough the probability for the particles to stay aligned is approximately the same as when they stay misaligned.

The main focus of Potts models is to find out the critical point and observe the phenomenon that occurs during the phase transition between order states. With square Lattice= 2 the critical point (usually denoted as T_c with T stands for "temperature" can be found mathematically (Schubert, 2008) as follows:(T in unit of J/K_β)

$$\boldsymbol{T_c} = \frac{\mathbf{1}}{\mathbf{\ln(1+\sqrt{q})}} \qquad \textbf{(3.12)}$$

Table 3.2: Critical points in systems with different number of states in the square Lattice= 2 (d=2)

q	T_c
2	1.135
3	0.995
4	0.91
5	0.852
10	0.70
100	0.40

For the sole purpose of presenting, the data was recorded from cold-start Potts models with value of all spin initialized to 0 at start. Unlike average energy which could only vary from 0 to 2, magnetisation varies from 0 to q - 1 and therefore the data presented in Figure (3.1) has been normalized to the range [0.0,1.0]. As can be observed the average magnetisation gradually increases toward the average value (0.5), and the models transform from magnetized to non-magnetized at the critical temperatures. This phenomenon occurs concurrently with the increase of energy from low to high.

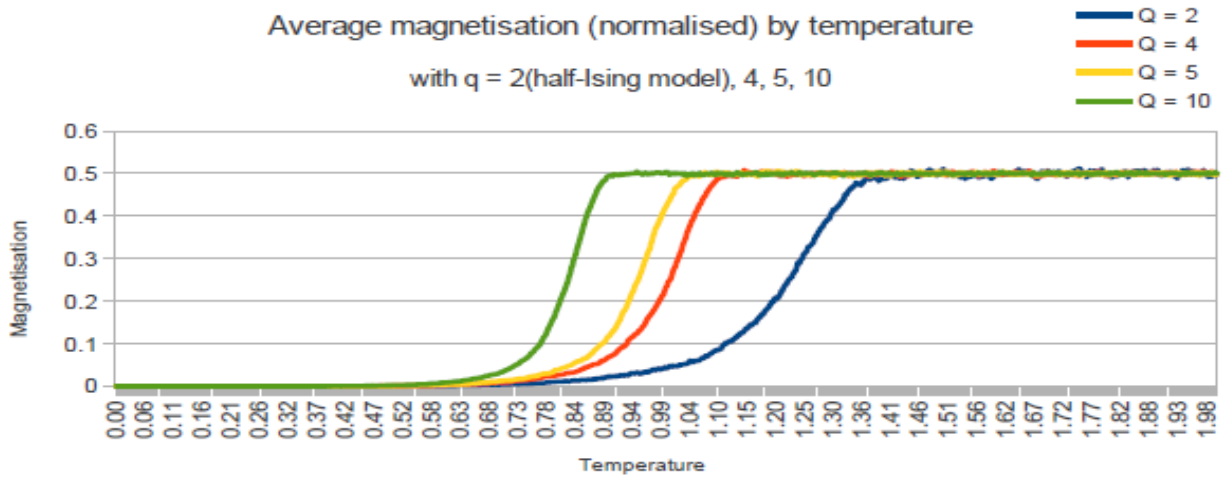

Figure (3.*1*): magnetisation of various Potts models when temperatures auto increment from 0.0 to 2.0. **(Tran, 2013)**

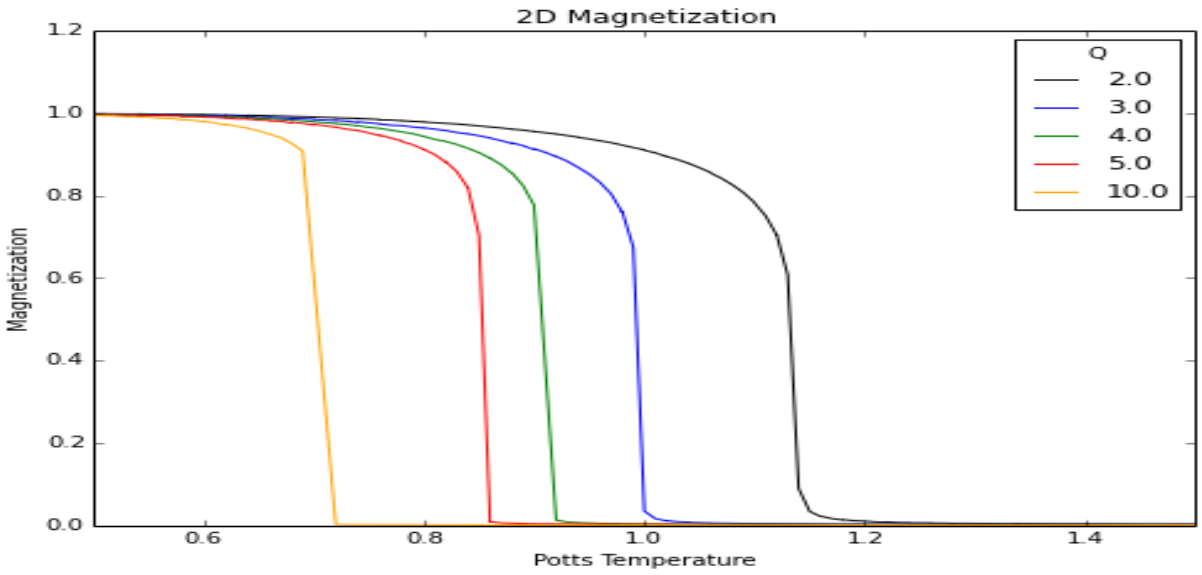

Figure (*3.2*): show the relation between magnetisation various temperatures for largest size lattice. **(Kurinsky, 2015)**

In figure (3.2) note the sharp discontinuities in higher spins and higher dimensions, and the difference between the d2, q=2 transition and the transitions at higher order, as well as the difference between the d=2, q=3 transition and the other q=3 transitions (it is, just barely, continuous; there is a slope and it does not go directly to 0). This is a significant effect, as it was seen for all lattices, and what it plotted is a lattice 1000 sites per side.

3.4. Applications for Potts Model

We find out three unique applications of the Potts model. The first is a physical application in which the Potts model is used to simulate the behavior of foams. The second is a biological application which simulates the growth patterns of tumors. The final example is a sociological example where the Potts model is used to study human interactions.

In these applications the Hamiltonian will become a little more complex to capture external factors. These use the following Hamiltonian.

$$\boldsymbol{H = \ -J \sum_{<ij>} \delta_{\sigma_i, \sigma_j} \ - h \sum_i \sigma_i \ .} \qquad \textbf{(3.13)}$$

In this case the strength of the interaction between neighboring elements ***J*** varies depending on their location on the lattice. The second sum is the addition of an outside force which also depends on the position within the lattice. **(Beaudin et al., 2010)**

a- <u>Physical application:</u>

The first experiment is described by Sanyal et al (Sanyal & Glazier, 2006) in their article titled, "Viscous instabilities in flowing foams: A Cellular Potts Model." This experiment tracks a single large bubble as it flows through a foam. At first glance, foam flow may not seem to have many applications. However, "foams are of practical importance in applications as diverse as brewing, lubrication, oil recovery, and firefighting" (Jiang, 1996) Foams exist in many dangerous and challenging fields. The Hamiltonian for the experiment takes into consideration the energy of this system as well as the area of the bubbles. $\boldsymbol{H = \ \sum_{<ij>} J\ (1 - \delta_{\sigma_i, \sigma_j}) + \lambda \sum_n (a_n - A_n)^2}$ **,** **(3.14)**

The variable **λ** is the strength of the area constraint on the bubble. The unattainable value $\boldsymbol{A_n}$ is the area the bubble would assume if there were no forces acting on it, and $\boldsymbol{a_n}$ is the current area of the same bubble. The counter *n* is the number of bubbles.

b- <u>Biological application</u>

The second application involves studying a cancerous tumor. Sun *et al(Sun, Chang, & Cai, 2004)* describe their experiment in the article titled "A Discrete Simulation of Tumor Growth Concerning Nutrient Influence." The authors use the Potts model to determine whether the amount and location of nutrients affect the growth pattern of a tumor.

CHAPTER FOUR

UNUSUAL FERROMAGNETISM IN ISING AND POTTS MODEL ON SEMI-DIRECTED BARABÁSI-ALBERT NETWORKS

4.1. Introduction

4.2. Semi-Directed Barabási-Albert Networks

4.3. Model and Simulation

4.3.1. The Versions SDBA1 and SDBA2
4.3.2. Ising Model On SDBA Networks
4.3.3. Potts Model On SDBA Networks

4.4. Results and Discussion

4.4.1. Ising Model

4.4.2. Potts Model

CHAPTER FOUR

UNUSUAL FERROMAGNETISM IN ISING AND POTTS MODEL ON SEMI-DIRECTED BARABÁSI-ALBERT NETWORKS

4.1. Introduction

The Ising and Potts model were used to test and improved algorithms to calculate the important foundations of high precision for the calculation of critical exponents in equilibrium statistical mechanics using a new Monte Carlo methods, including: Metropolis (Merton, 1968); Swendsen-Wang (Swendsen & Wang, 1987), Wang-Landau (Wang & Landau, 2001). The Ising model was applied to expand the undirected Barabási-Albert networks (UBA), so that was simulated by Monte Carlo methods which refers to indicate a Curie temperature increasing logarithmically with increasing system size ($\boldsymbol{T_c \propto N}$). Differently from (Aleksiejuk et al., 2002), Sumour et al. (M. A. Sumour & Shabat, 2005),(M. A. Sumour et al., 2005) studied the Ising model on a directed Barabási-Albert network (DBA) using standard *Glauber kinetic Ising models* on fixed networks. They confirmed the asymptoptic Arrhenius extrapolation ($\boldsymbol{\ln \tau \propto T}$) [1]for the time $\boldsymbol{\tau}$ until the first sign change of the magnetisation, meaning that at all finite temperatures the magnetization eventually vanishes (M=0)

This chapter, studying the critical behavior of Ising and Potts model on semi-directed Barabási-Albert network (SDBA), where now the number **N(k)** of nodes with **k** links each decays as $\boldsymbol{N(k) \sim \frac{1}{k^{-\gamma}}}$ and the exponent $\boldsymbol{\gamma}$ decreases from 3 to 2 for increasing $\boldsymbol{m}$ where $\boldsymbol{m}$ is the number of old nodes, which a new node, added to the network, selects to be connected with. This behavior is totally different from UBA and DBA scale-free networks, where $\boldsymbol{\gamma}$ = 3 is universal, i.e., independent of $\boldsymbol{m}$. For both Ising and Potts model in our results no usual phase transition has been found, similar to (Aleksiejuk et al., 2002), (M. A. Sumour et al., 2005)

4.2. Semi-Directed Barabási-Albert Networks

Both UBA and DBA networks are grown such that the probability, of a new site to be connected to one of the already existing sites, is proportional to the number of previous connections to this already existing site: the rich get richer.

In this way, each new site selects exactly ***m*** old sites as neighbours. In a UBA network (Aleksiejuk et al., 2002), the neighbour relations for the spin interactions were such that if **A** has **B** as a neighbour, **B** has **A** as a neighbour, while, for DBA, in general **B** then does not have **A** as a neighbour.

In the DBA and UBA networks (M. A. Sumour & Shabat, 2005),(M. A. Sumour et al., 2005),if a new node selected ***m*** old nodes as neighbours, then the ***m*** old nodes are added to the Kert´esz list and the new node is also added ***m*** times to that list. Connections are made with ***m*** randomly selected elements of that list. If one only added the old nodes to the list, then only the initial core would be selected as neighbours, which is not interesting. But if one adds to the list the ***m*** old nodes plus once the new node, one has a semi-directed network: **SDBA**. (For usual BA networks, the new node is added ***m*** times to the Kert´esz list.)

4.3. Model and Simulation

4.3.1 The versions SDBA1 and SDBA2

Our first version, SDBA1, builds the network in the way of (M. Sumour & Radwan, 2012). The new node ***n*** selects ***m*** sites ***j***, which ***n*** will all influence, while ***n*** will be influenced only by the first selected ***j.*** Our second version, SDBA2, inverts the direction of the spin interaction: The new node ***n*** selects ***m*** sites ***j***, which will all influence ***n***, while ***n*** will influence only the first selected ***j***.

Networks simulated with ***N*** nodes ***i*** , with spins S_i on each node. For both Ising and Potts model on SDBA, the evolution in time is given by single spin-flip Glauber dynamics with a probability ***P*** given by *Appendix 4*

$$P = 1/[1 + \exp\left(\frac{2\nabla E}{K_B T}\right)] \quad (4.1)$$

with ∇E to be defined below through eqs. (4.2) and (4.3). Here, the time is defined as one Monte Carlo step (MCS), where one MCS is accomplished after all N spins are updated; and we denote the final Monte Carlo step number as **MCSN**. (like number of iterations for equilibration.)

The error bars [3]are usually smaller than the size of symbols, so cannot put them into the figures. The statistical errors were evaluated from 10 to 100 samples of initial configurations and with 4000 to 100000 Monte Carlo steps (thermal error).

4.3.2. Ising Model On SDBA Networks

The Ising interaction energy is given by

$$H = -J \sum_i \sum_j s_i \, s_j \quad (4.2)$$

where $s_i = \pm 1$, and the inner sum runs over all neighbours j of node i. And the magnetisation defined for this model as:

$$M_v = \frac{\sum_{i=1}^{N} s_i}{N} \quad . \quad (4.3)$$

(M. A. Sumour et al., 2005)

[3] **Error bars** are a graphical representation of the variability of data and are used on graphs to indicate the error, or uncertainty in a reported measurement. They give a general idea of how precise a measurement is, or conversely, how far from the reported value the true (error free) value might be. Error bars often represent one standard deviation of uncertainty, one standard error, or a certain confidence interval (e.g., a 95% interval). These quantities are not the same and so the measure selected should be stated explicitly in the graph or supporting text*.(Bertini, Kennedy, & Puppo)

4.3.3. Potts Model On SDBA Networks

In the Potts model, the interaction energy is written as:

$$H = -J \sum_i \sum_j \delta_{s_i, s_j} \quad , \tag{4.4}$$

with δ_{s_i, s_j} *Kronecher's* delta and s_i = 1, 2, . . . q. Again, to study the critical behaviour, the magnetisation is defined as:

$$M_v = \frac{(qM-N)}{[(q-1)N]} \quad , \tag{4.5}$$

where **M** is the largest of the q numbers of spins s_i in one of the q directions 1, 2, . . ., q, at each iteration. **(M. Sumour & Radwan, 2012)**

4.4. Results and Discussion

4.4.1. Ising Model

Using the FORTRAN program as in our appendix 3, with different ***m***. The number of nodes ***N*** added to the initial core of ***m*** nodes is 10000 to 50000, and **MCSN** = 100000 iterations were made. First we measure the number ***N(k)*** of nodes influenced by ***k*** neighbours in SDBA2, analogous to (M. Sumour & Radwan, 2012) for SDBA1. In **fig. (4.1)**, for each ***m*** value (including ***m*** = 1, not shown), plotting double-logarithmically the observed numbers of nodes with at least ***k*** links each and determined the decay exponents by the slopes $\gamma(m) - 1$ versus 1/***m***, which makes the possible extrapolation towards infinite ***m*** (***m*** = ∞, 1/***m*** = **0**) clearer. Maybe the true exponents $\gamma(m)$ equal ***2+1/m***, since ***m = 1*** should give the standard (undirected) exponent γ **= 3**. The deviations from this formula (straight line in fig. (4.1)) are not much larger than our systematic errors. As an alternative to the linear behaviour also a power-law fit to ***m*** > 1 is shown. We see that the new power-law fit agrees very nicely with the data except for the standard BA model

(undirected) case ***m = 1***. The behaviour of the exponents for much larger ***m*** is discussed elsewhere (Choudhury et al., 2014) and differs appreciably between SDBA1 and SDBA2.

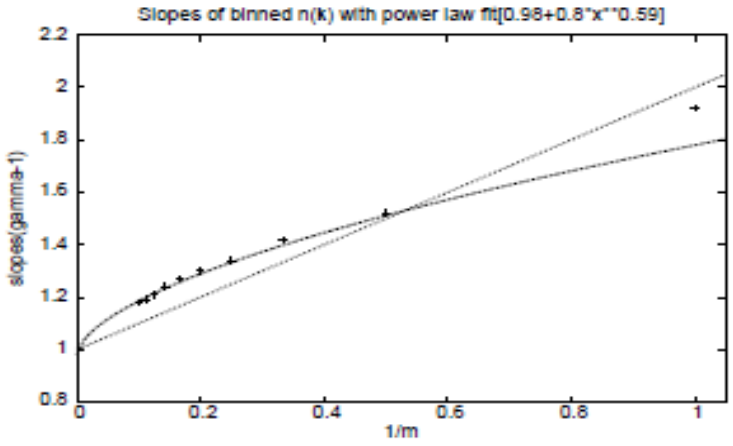

Figure (4.1): Plot of ɤ(m) − 1 versus 1/m with power –law: ɤ-1 = 0.98+0.8/m0.59, N=4100000 nodes (M. Sumour & Radwan, 2012)

Figure (4. 2) shows the magnetisation as a function of temperature (T = 0, 1, 2, . . ., 16). The roughly exponential decay is similar to (Aleksiejuk et al., 2002) Then changed the initial number of neighbours ***m*** = 1, 3, 5, 7 with system size ***N=50000*** and **MCSN** = 4000 to 100000 iterations.

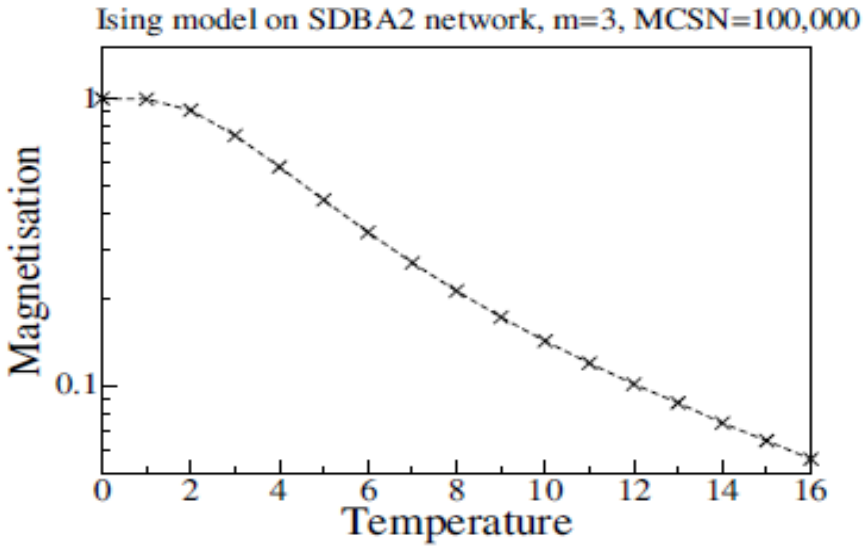

Figure (4.2): Semi – logarithmic plot of magnetisation versus T for m= 3 and 400 nodes. (M. Sumour & Radwan, 2012)

In fig. (4.3) we see that with decreasing ***N***, the magnetisation is decreasing except that at small temperatures, the magnetisation does not change.

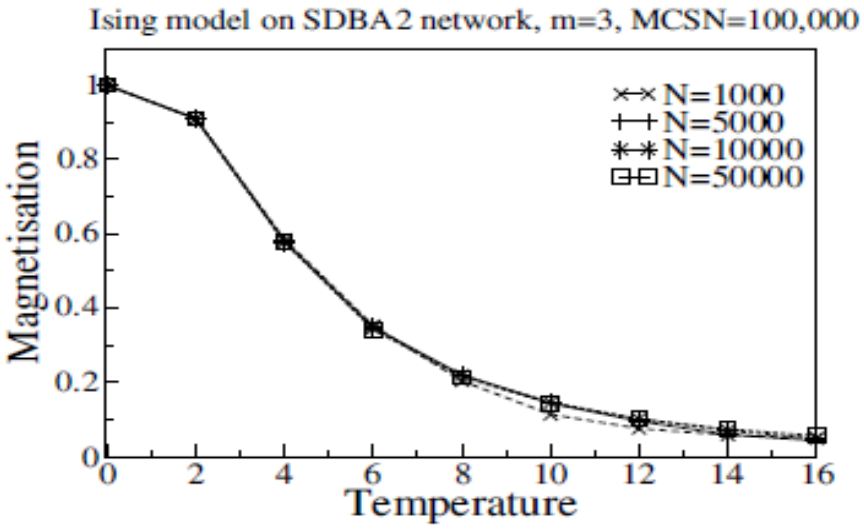

Figure (4.3): Plot of magnetisation versus T for m= 3 and different system sizes N=1000 to 50000, MCSN = 100000. (M. Sumour & Radwan, 2012)

4.4.2. Potts Model

To study the q = 2 Potts model we start with all spins ordered S = 1, a number of spins equal to N = 500, 5000,50000, and 100000 with MCSN = 10^8, 10^7 and 2×10^6 with Heat Bath algorithm, respectively, in **figs. (4. 4)(a), (b), (c) and (d).**

The temperature is measured in units of **J/kB**[4]. We determine the time τ after which the magnetisation has flipped its sign for first time, and then take the median value of 9 samples. So, this way, it is possible to determine various temperatures for different network sizes and to extrapolate τ to infinity and obtain the critical temperature for SDBA1 and SDBA2 networks. simulations on SDBA1 and SDBA2 networks indicate that the q = 2 Potts model does not display a usual phase transition and the plots of the time **1/ ln(τ)** versus temperature in **figs.(4. 4)(a**), **(b), (c) and (d)** show that the results agree with the

[4] k_B = 1.380658 x 10^{-23} J/K, implying that J/k_B = 1

Vogel-Fulcher-Tammann law[5] for the relaxation time τ , defined as the first time, when the sign of the magnetisation flips: $\mathbf{1/\ln(\tau) \propto T - T_c(N)}$. We extrapolate $T_c(N)$ for N logarithmically with N as in (Aleksiejuk et al., 2002)

Table (4.1): the data is the value of $T_c(N)$ versus the different number of N for SDBA1 and SDBA2

SDBA1									
N	**20**	**30**	**50**	**100**	**200**	**500**	**5000**	**500000**	**100000**
$T_c(N)$	**0.1**	**0.2**	**0.7**	**1.0**	**1.1**	**1.3**	**3.1**	**5.3**	**6.0**
SDBA2									
$T_c(N)$	**0.5**	**0.7**	**1.0**	**1.5**	**1.8**	**2.5**	**4.2**	**6.6**	**7.0**

[5] **the Vogel-Fulcher-Tammann (VFT) law**:

The Vogel-Fulcher-Tammann (VFT) equation has been used extensively in the analysis of the experimental data of temperature dependence of the viscosity or of the relaxation time

$$\tau = \tau_o \exp(A/(T - T_o))$$

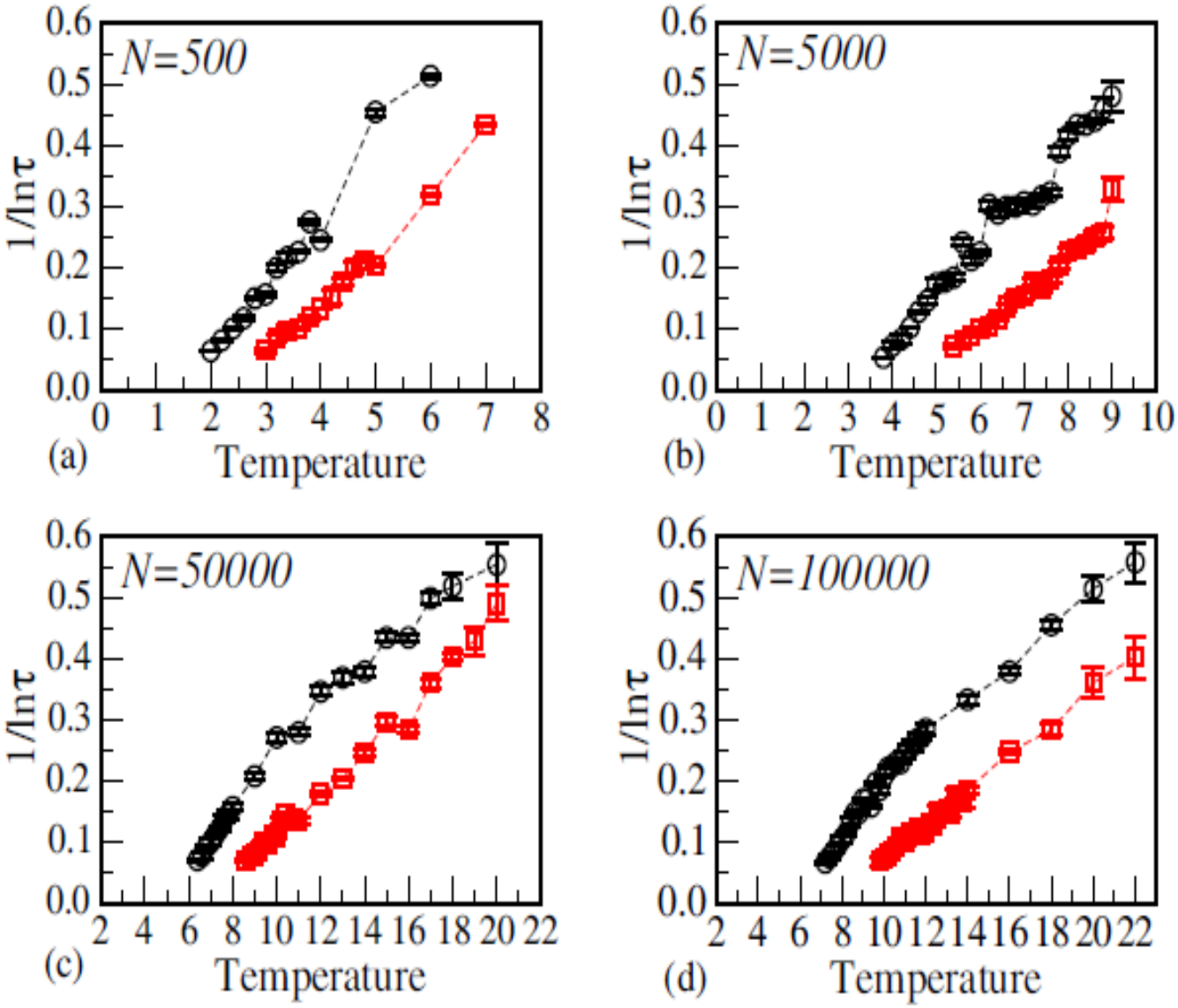

figure (4.4): Reciprocal logarithm of the relaxation time versus temperature for SDBA1(circle) and SDBA2(square) networks and Potts model with q = 2 (Ising), m= 2 and 400 nodes initial neighbours and N =500(a),5000(b),50000(c), and 100000(d) sites. (M. Sumour & Radwan, 2012)

Fig. (4. 5) show the magnetisation versus temperature behaviour on SDBA1 and SDBA2 networks for the Potts model with ***q = 2*** states and ***m*** = 3 initial neighbours and ***N*** = 50000 sites. Both SDBA1 and SDBA2 network present similar behaviour, but SDBA1 decreases faster than SDBA2 with increasing temperature, since SDBA2 has more neighbours than SDBA1. Two different programs using for Potts and Ising, which agree in their results for ***q = 2***, and they should.

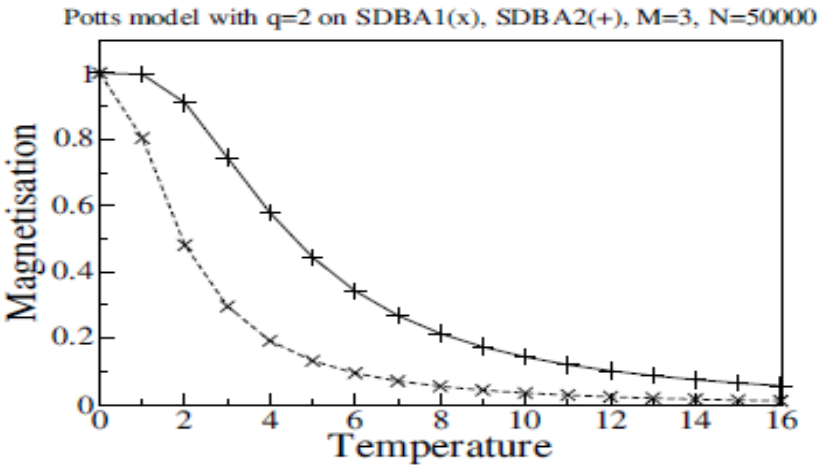

Figure (4.5): Plot of the magnetisation versus temperature for SDBA1(x) and SDBA2(+) networks and Potts model with q = 2, m=3 initial neighbours and N =50000 sites and MCSN = 100000 iterations**.** (M. Sumour & Radwan, 2012)

Fig. (4. 6) illustrates the magnetisation versus the temperature on SDBA1 network for the Potts model with **q** = 2, 3, and 10 states, ***m*** = 3 initial neighbours and ***N*** = 50000 sites. Here, we see that increasing **q** of the Potts model provides a more rapid decay of the magnetisation as a function of temperature.

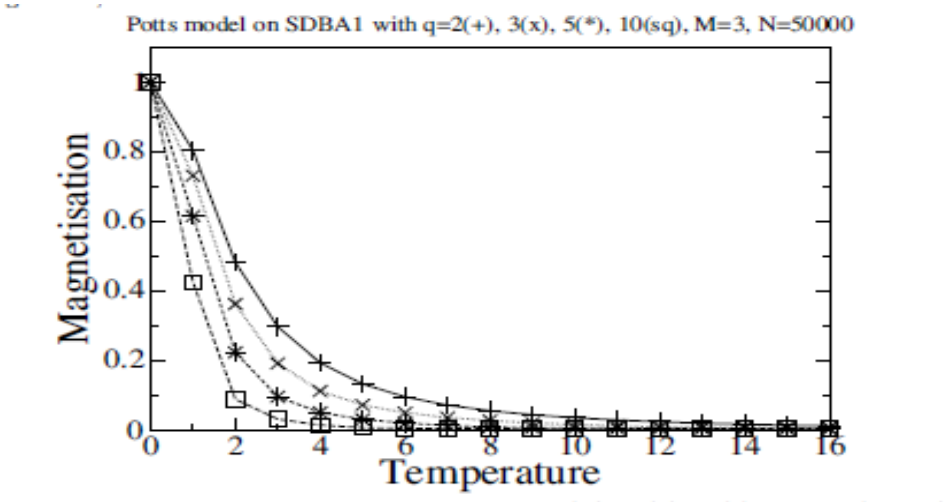

Figure (5.6): Plot of the magnetisation versus temperature for different values of q = 2(+), 3(x) ,5(*), and 10(square) on SDBA1networks for N =50000 sites and m=3.

(M. Sumour & Radwan, 2012)

In fig. (5.7), we show the same behaviour, we see that increasing **q** of the Potts model provides a more rapid decay of the magnetisation as a function of temperature. but now on the SDBA2 network.

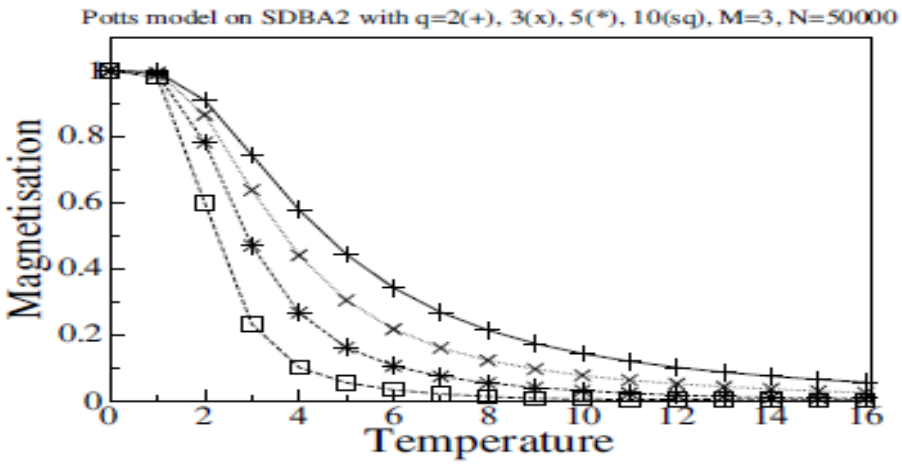

Figure (5.7): Plot of the magnetisation versus temperature for different values of q = 2(+), 3(x) ,5(*), and 10(square) on SDBA2networks for N =50000 sites and m=3.

(M. Sumour & Radwan, 2012)

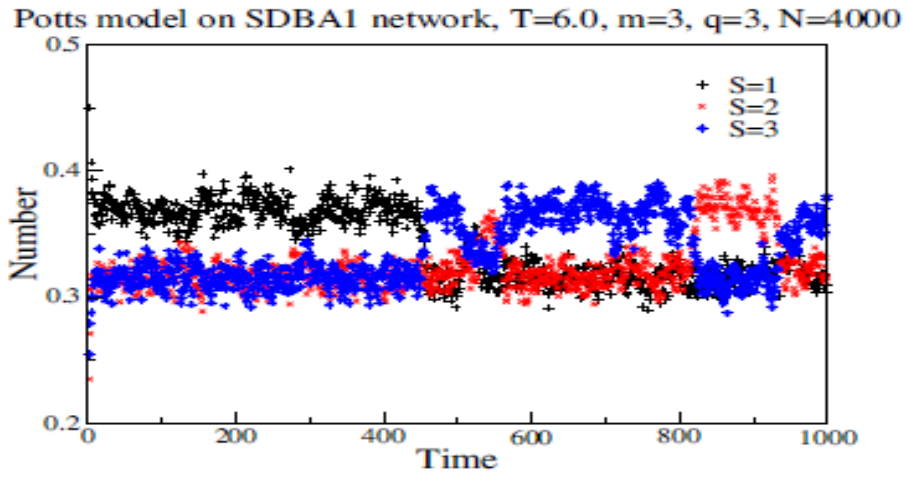

Figure (4.8): Plot of the number of S=1,2 and 3 states versus the time for the Potts model with q=3 states on SDBA1network, for m=3 , N =4000 (M. Sumour & Radwan, 2012)

In fig. (4.8) we show the time dependence of the number of S = 1 and 3 states for the Potts model with ***q = 3*** states on SDBA1 network. Here we observe the tunneling between these three states with the evolution of time. In fig. (4. 9) we show the same behaviour as in fig. (4.8), but now on the SDBA2 network.

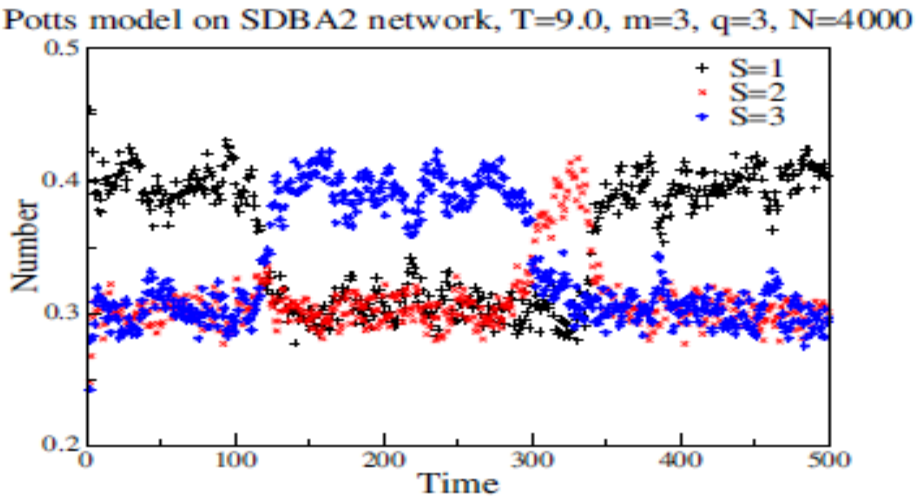

Figure (4.9): Plot of the number of S=1,2 and 3 states versus the time for the Potts model with q=3 states on SDBA2network, for m=3, N =4000. **(M. Sumour & Radwan, 2012)**

CHAPTER FIVE

FINITE-SIZE EFFECTS ON SEMI-DIRECTED BARABÁSI-ALBERT NETWORKS

CHAPTER FIVE

FINITE-SIZE EFFECTS ON SEMI-DIRECTED BARABÁSI-ALBERT NETWORKS

5.1. Introduction

The construction of a Barabási-Albert network (BA)(Adamic & Huberman, 2000),(Aleksiejuk, Hołyst, & Stauffer, 2002) presents two important concepts: the growth of the network and preferential attachment. Starting with a core of m nodes, one after another each new node connects to m already existing nodes, until N nodes were added to the initial core. The growth means that the number of nodes in the network increases over time and preferential attachment means that the more connected a node is, the more likely it is to receive new links.

Then BA is growing such that the probability of a new site to be connected to one of the already existing sites, is proportional to the number of previous connections to this already existing site: The rich gets richer. In this way, each new site selects exactly m old sites as neighbors. In directed (DBA) and undirected (UBA) Barabási- Albert networks, the network itself was built in the standard way, but when agents (spins) were put on the network nodes (Aleksiejuk, Hołyst, & Stauffer, 2002);(M. A. Sumour & Shabat, 2005);(M. A. Sumour, Shabat, & Stauffer, 2005) ;(Lima, 2015) the neighbor relations were such that if A has B as a neighbor, B in general does not have A as a neighbor for DBA while it does have for UBA. Differently, semi-directed BA networks (SDBA) have directedness already in their growth and attachment process and do not require agents on their nodes (Stauffer, 2015) ;(M. A. Sumuor, 2015) The present work continues the study of two semi-directed BA networks, SDBA1(M. Sumour et al.) and SDBA2(M. A. Sumour & Lima, 2014) for much larger m and checks effects of finite size N on these networks with $2 \leq m \leq 300$.

5.2. Model and Simulations

5.2.1. Undirected Barabási-Albert Network

The undirected Barabási-Albert network (Adamic & Huberman, 2000),(Aleksiejuk et al., 2002) is grown such that the probability of a new node to be connected to one of the already existing nodes is proportional to the number of the previous connections to this already existing node: the rich get richer. In this way, each new node selects exactly m old nodes as neighbors. If a new node selects randomly m old nodes as neighbors, then the m old nodes are added to a long array of node indices called the Kert'esz list, and the new node is also added m times to that list. At the start of the network growth, this Kert'esz list is empty. The above random selections are made by selecting m random nodes from the Kert'esz list. The neighbor relations were such that if A has B as a neighbor, B has A as a neighbor.

5.2.2. Directed Barabási-Albert Network

In directed Barabási-Albert networks, the network itself is produced in the undirected Barabási-Albert networks way. When interacting agents are put onto this network, each node is influenced by the fixed number m of neighbors with it had selected when joining the network. It is not influenced by other nodes that selected it as neighbor after it joined the network, i.e., the neighbor relations were such that if A has B as a neighbor, B in general does not have A as a neighbor in the later interactions of agents on this DBA network.

5.2.3. Semi-Directed Barabási-Albert Network (SDBA)

The semi-directed Barabási-Albert networks version is constructed similarly to the undirected Barabási-Albert network. When a new node makes connections with m randomly selected old nodes of the Kert'esz list, one adds the m old nodes, plus only once (and not m times), the new node; then one has a semi-directed network. For SDBA we have two versions SDBA1 and SDBA2:

a- Semi-directed Barabási-Albert networks (SDBA1):

Our first version, SDBA1, the new node n selects m nodes j, which n will all influence, while n will be influenced only by the first selected j.

b- Semi-directed Barabási-Albert networks (SDBA2):

Our second version, SDBA2, inverts the direction of the node interaction: The new node n selects m nodes j, which will all influence n, while n will influence only the first selected j.

In summary, UBA and DBA have the same network, and only the later interactions between agents (spins) put onto these networks differ. SDBA networks, in contrast, differ already in their structure and need no agents to make this difference visible.

5.3. Results and Discussion

Let $\boldsymbol{K_c = \sum_{i=1}^{m} K(i)/m}$ **and** $\boldsymbol{K_n = \sum_{i=m+1}^{m+N} K(i)/m}$ **,**

be the average number $\boldsymbol{K_c}$ of neighbors $\boldsymbol{K(i)}$ influencing one of the $\boldsymbol{m}$ core nodes and $\boldsymbol{K_n}$ an analogous quantity for the $\boldsymbol{N}$ non-core nodes added to the core. In the simulations, two codes for SDBA1 and SDBA2 networks were used as in appendix (1-2) (M. Sumour et al); (M. A. Sumour & Lima, 2014)The Fig(5.1) and (5.2) were built from the tables (5.1) and (5.2), respectively, for SDBA1 and SDBA2 networks. These show the average number of neighbors ($\boldsymbol{K_c}$) with $\boldsymbol{m}$ = 2; 15, and 100, versus $\boldsymbol{N}$ = 10^3 to 2 * 10^7. From both tables and figures (1 and 2) and for m = 100 we have the effect of finite size up to N = 4000000 nodes for both SDBA1 and SDBA2.

These data show that SDBA1 gives very nice straight lines, while SDBA2 does only for m = 2 and 15 and not for m = 100. This is an important difference between the two networks in the effect of finite-size. The behavior for $\boldsymbol{K_n}$ is different, due to a change in

the loop 6 of the main code, replacing $\boldsymbol{K_c}$ by $\boldsymbol{K_n}$. We sum all $\boldsymbol{K(i)}$ from $\boldsymbol{i = m + 1}$ to $\boldsymbol{i = m + N}$ while Figs. (5.1) and (5.2) summed from $\boldsymbol{i = 1}$ to $\boldsymbol{i = m}$.

Table (5.1): Average number of core neighbours ($\boldsymbol{K_c}$) ,for *m*= 2,15and100 from SDBA1, versus different number of N of nodes

N	**m=2**	**m=15**	**m=100**
	Average neighbours (K_c)	**Average neighbours (**K_c)	**Average neighbours (**K_c)
1000	159.5	849.1	1083.7
5000	465.0	3764.7	4956.9
10000	745.5	7205.2	9754.0
20000	1195.5	13762.9	19284.2
50000	2225.0	32484.9	47635.7
100000	3525.0	62141.5	94539.1
500000	10332.0	280725.7	464831.4
1 Million	16398.8	537837.38	923198.63
2 Million	26131.0	1030183.1	1833653.8
4 Million	41537.0	1972485.4	3642164.5
5 million	48203.5	2431307.8	-
10 Million	76375.0	-	-
20 Million	121224.5	-	-

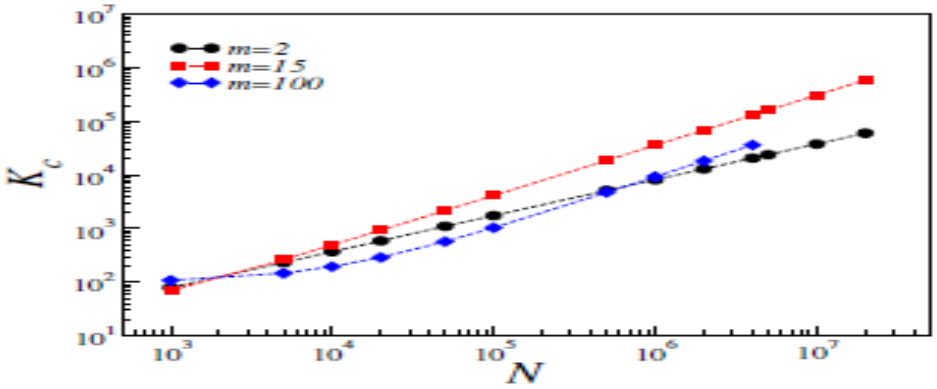

Figure 5.1: Average number of core neighbours (K_c) ,for m= 2,15and100 from SDBA1, versus N =1000 to 20million of nodes. See table (5.1)**_(Radwan, Sumour, Elbitar, Shabat, & Lima, 2016)**

Table (5.2): Average number of core neighbours (K_c) ,for *m*= 2,15and100 for SDBA2, versus different number of N of nodes:

N	**m=2**	**m=15**	**m=100**
	Average neighbours (K_c)	**Average** neighbours (K_c)	**Average** neighbours (K_c)
1000	79.5	69.8	108.8
5000	233.0	264.5	147.4
10000	372.5	495.6	195.3
20000	592.5	934.5	290.4
50000	1107.0	2182.3	573.8
100000	1749.5	4150.9	1042.2
500000	5172.0	18752.3	4743.2
1 Million	8173.5	36241.3	9325.4
2 Million	13004.5	68790.7	18430.8
4 Million	20680.5	131622.3	36518.9
5 million	24003.0	162229.1	-
10 Million	38096.0	310610.9	-
20 Million	60532.5	594663.9	-

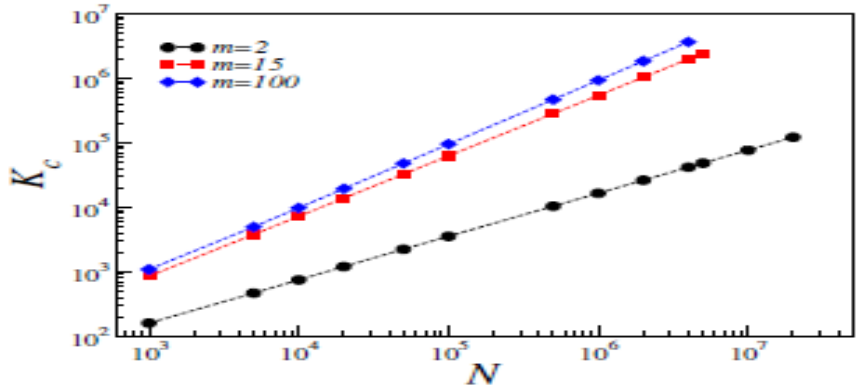

Figure 5.2: Average number of core neighbours (K_c) ,for *m*= 2,15and100 from SDBA2, versus N =1000 to 20million of nodes. See table (5.2) **(Radwan, Sumour, Elbitar, Shabat, & Lima, 2016)**

Thus we change in the codes the loop 6 into ***i = 1+m***; max to get K_n . For this non-core K_n versus ***N*** for ***m*** = 2; 15, and 100 for SDBA1 and SDBA2 in our log-log plots (not shown), in contrast to Figs (5.1) and (5.2), all the data lie on straight lines having the same slope. Thus instead *Figs(5.3) and (5.4)* show the ratio K_n /***N*** (linear scale) versus ***N*** (logarithmic scale), giving only minor variations with ***N***.

Table (5.3): The data is the value of the ratio K_n /*N* from SDBA1 versus different number of lattice size *N* with three values of m= *2,15,100.*

N	***m=2***	***m=15***	**m=100**
	K_n /***N***	K_n /***N***	K_n /N
5000	1.407	*0.3165*	0.0384
10000	1.425	*0.*3475	*0.*0445
50000	*1.455*	0.4172	0.0593
100000	1.464	*0.*44539	*0.*0655
1000000	1.4836	*0.*52884	*0.*0869
2000000	1.4869	0.55158	0.0904
4000000	1.4896	0.55226	0.0938

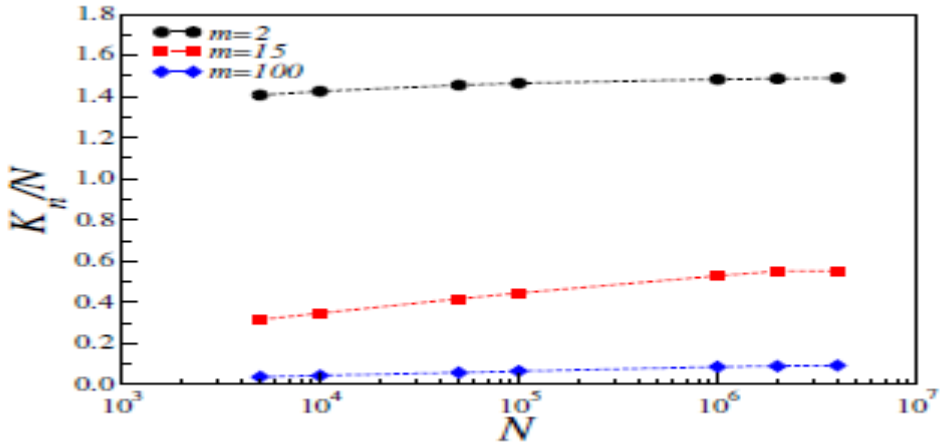

Figure (5.3): ratio K_n/N from SDBA1 versus different number of lattice size *N* with three values of m= *2,15,100* **. (Radwan, Sumour, Elbitar, Shabat, & Lima, 2016)**

Table (5.4): The data is the value of the ratio $\mathbf{K_n}$ /N from SDBA2 versus different number of lattice size N with three values of m = *2,15,100*

N	***m=2***	**m=15**	**m=100**
	K_n/N	$\mathbf{K_n}$ /N	$\mathbf{K_n}$ /N
5000	*1.4536*	1.016	1.0073
10000	1.4*628*	1.018	1.0074
50000	*1.4778*	1.0233	1.0005
100000	1.4*825*	1.0253	1.00056
1000000	1.4*918*	1.0307	0.9876
2000000	*1.4935*	1.0638	0.97467
4000000	*1.4948*	1.0813	0.968193

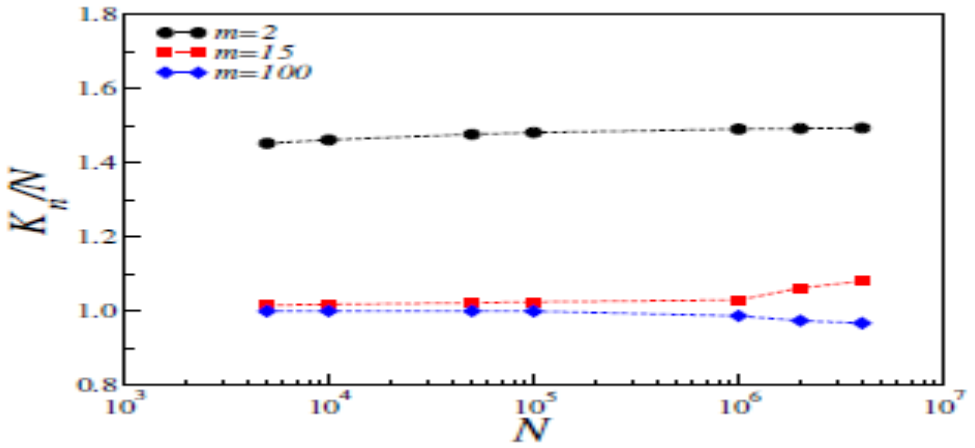

Figure (5.4): The ratio K_n /*N* from SDBA2 versus different number of lattice size *N* with three values of m= *2,15,100.* **(Radwan, Sumour, Elbitar, Shabat, & Lima, 2016)**

*In the Figs (5. 5)and (5.6)*we plot the number $K(i)$ of neighbors versus node index i with i = 1; 2; : : :N = 10^6 for SDBA1 and SDBA2. These gives a clear gap in the number of $K(i)$ of neighbors. This gap occurs next to m = 100 and for m > 100 the $K(i)$ shrink drastically. For clarity, data above i = 1000 are binned.

A gap in the $K(i)$ plots of *Figs. (5.5)and(5.6),* and also in Ref. (M. A. Sumuor, 2015) Such an effect was already reported a decade ago in Ref. (Guimarães Jr, de Aguiar, Bascompte, Jordano, & Dos Reis, 2005) if the core is not connected completely but only partially (Erdos-Renyi network). This explanation does not fit SDBA with fully connected cores. For our simulations, in undirected Barabási- Albert networks (UBA) as well as in the two types SDBA1 and SDBA2 of semi directed networks, when the core has been constructed, each of the m core nodes appears m times in the Kert'esz list (called "list" in the programs). All the later added non-core nodes $i = m+1; m+2$; ……; $m+N$ after their addition are inserted m times to the Kert'esz list for UBA but only once for SDBA; see Section 2. Thus each SDBA core node has a roughly m times bigger chance than node $i = m+1$ to be selected by the later node $i = m + 2$. Therefore, between $i = m$ and $i = m + 1$ the number $K(i)$ of neighbors for very large m jumps down by a factor near m, as seen in

Figs. (5.5) and(5. 6) for $\boldsymbol{m}$ = 100. For small $\boldsymbol{m}$ like $\boldsymbol{m}$ = 2 this jump and the region to the left of the jump are much smaller and thus barely visible.

Fig. (5.5) is different from **Fig. (5. 6)** by orders of magnitude For SDBA1 in **Fig.(5.5)** each non-core node n at the time it joined the network gets $\boldsymbol{K(n)}$ = 1 neighbors, while for SDBA2 in Fig. **(5. 6)** it gets $\boldsymbol{K(n)} = \boldsymbol{m}$ neighbors influencing it. During the later growth of the network, in both SDBA1 and SDBA2 the $\boldsymbol{K(i)}$ can increase but this initial difference still has a visible effect: $\boldsymbol{K(i)}$ can go down to unity in SDBA1 but is at least m for SDBA2.

For SDBA1 each of the **N** non-core nodes selects $\boldsymbol{m}$ neighbors, mostly from the $\boldsymbol{m}$ core nodes, and thus at the end each core node was selected roughly **N** times in **Fig.(5. 5)**: $\boldsymbol{K(i)} \cong 10^6$ for $\boldsymbol{1 \leq i \leq m}$. For SDBA2 each of the **N** non-core nodes instead selects only one neighbor, again mostly from the core. Thus for the core nodes $\boldsymbol{K(i)} \cong \boldsymbol{N=m} = 10^4$, as seen in the left part of **Fig. (5.6).**

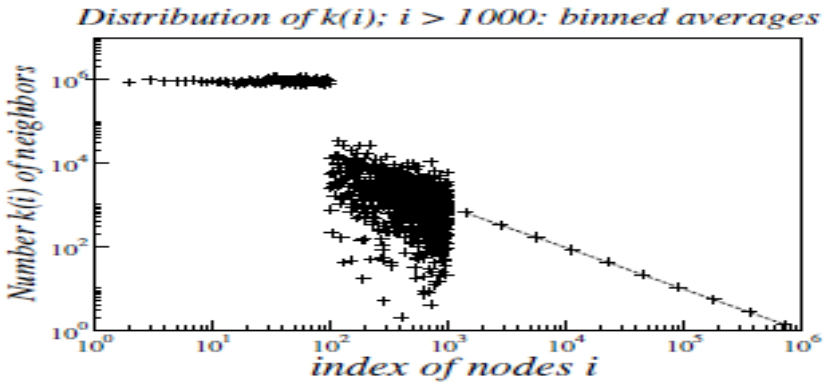

Figure (5.5): Number $\boldsymbol{K(i)}$ of neighbors influencing node *i* versus node index with *i* = 1; 2; …. N at m= *100* and N=one million , from SDBA1 . **(Radwan, Sumour, Elbitar, Shabat, & Lima, 2016)**

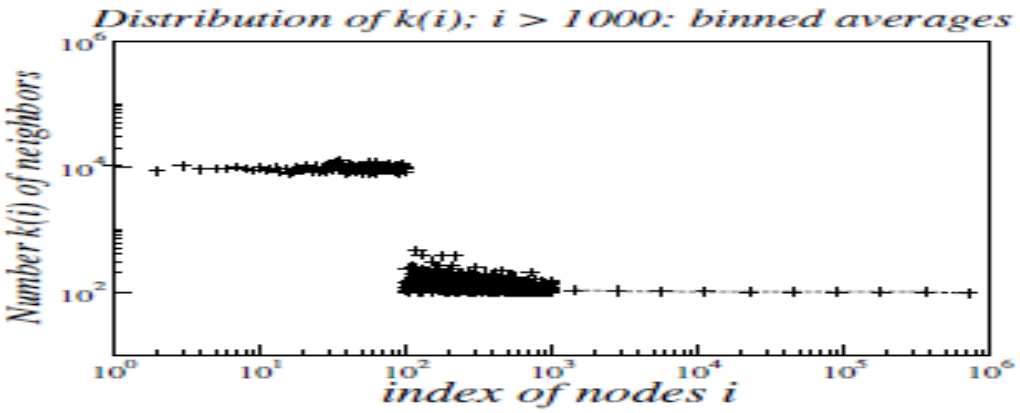

Figure (5.6): Number $K(i)$ of neighbors influencing node i versus node index with i = 1; 2; …. N at m= 100 and N=one million, from SDBA2. **(Radwan, Sumour, Elbitar, Shabat, & Lima, 2016)**

The $\boldsymbol{K_c}$ and $\boldsymbol{K_n}$ are plotted *in the Figs(5.7) and (5.8)* versus ***m*** for SDBA1 and SDBA2, averaged over 100 samples. Again, for *Fig(5.8)* the behavior of $\boldsymbol{K_n}$ is different of $\boldsymbol{K_c}$, due to a change in the loop 6 of the main code, as explained above .

Table (5.5): the data is the value of average number $\boldsymbol{K_c}$ of neighbors for *m* core nodes (i= 1, 2….., *m*) versus different number of m for SDBA1 and SDBA2 at N= 10^6

m	$\boldsymbol{K_c}$ *core (average number (sum/**m**)*	
	SDBA1	*SDBA2*
2	16398.0	8173.5
4	93065.5	23233.3
8	304058.5	38034.8
15	537837.4	35916.5
32	759266.0	23751.6
64	878753.6	13798.9
100	923198.6	9325.4
128	939726.6	7469.1
256	972478.3	4052.6

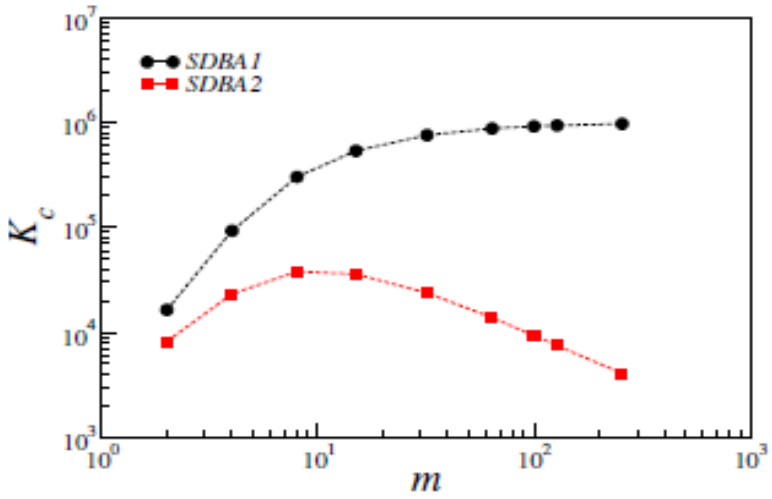

Figure (5.7): average number K_c of neighbors for *m* core nodes (i= 1, 2….., *m*) versus different number of *m* for SDBA1 and SDBA2 at N= 10^6 . **(Radwan, Sumour, Elbitar, Shabat, & Lima, 2016)**

Table (5.6): The data is the value of average number K_n of neighbors for *m* non-core nodes (i= 1, 2….., *m*) versus different number of m for SDBA1 and SDBA2 at N= 10^6

m	K_n *non- core(average number (sum/**m**)*	
	SDBA1	*SDBA2*
2	1483603.0	1491827.5
4	1156937.5	1226769.8
8	820948.5	1086972.3
15	528843.3	1030764.2
32	272015.13	1007373.0
64	136934.3	1001756.5
100	86900.6	987611.7
128	68212.8	1000404.1
256	31682.97	1000082.8

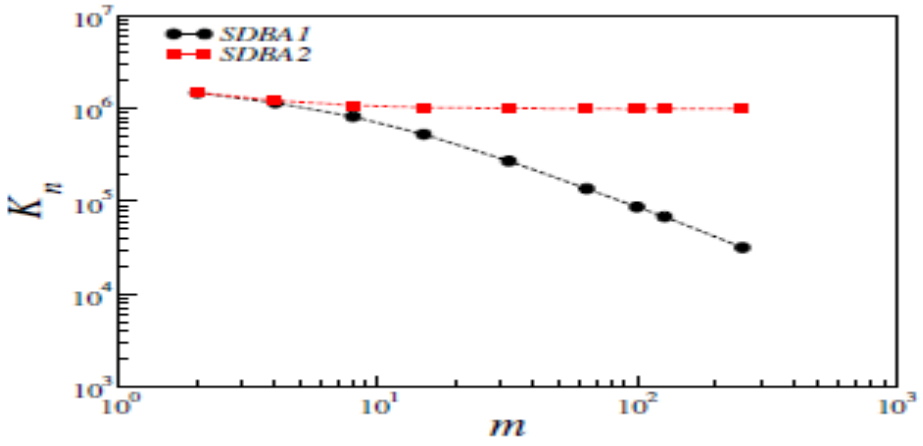

Figure (5.8): average number K_n of neighbors for *m* non-core nodes (i= 1, 2,…..,*m*) versus different number of *m* for SDBA1 and SDBA2 at N= 10^6 **. (Radwan, Sumour, Elbitar, Shabat, & Lima, 2016)**

Conclusion

There are many different models of interest in statistical mechanics, corresponding to the wide range of macroscopic systems found in nature and made in the laboratory.
Since 1999 the scale-free networks of Barabási-Albert have become very fashionable, and Ising spins have also been simulated on these Barabási-Albert networks.
So a special model in statistical mechanics ،as the Barabási-Albert networks ،will be discussed the Barabási-Albert (BA) or scale-free networks are very famous since 1999 and have been more recently modified into semi-directed (SDBA) networks.
The Barabási -Albert network is growing such that the probability of a new site to be connected to one of the already existing sites is proportional to the number of previous connections to this already existing site: The rich get richer. In this way, each new site selects m old sites as neighbours.
In directed Barabási- Albert networks, the network itself was built in the standard way, but when agents (spins) were put on the network nodes, the neighbour relations were such that if A has B as a neighbour, B in general does not have A as a neighbour. But in undirected Barabási-Albert network B has A as a neighbour.

In the undirected Barabási-Albert network, if a new node selects m old nodes as neighbours, then the m old nodes are added to the Kert'esz list, and the new node is also added m times to that list. Also in our semi-directed version, the new node makes connections with m randomly selected old nodes of the Kert'esz list. If one would only add the old nodes to the list, then only the initial core can be selected as neighbours, which is less interesting. But if one adds to the list the m old nodes, plus only once (and not m times) the new node, then one has what we call here a semi-directed Barabási-Albert network (SDBA). We deal here only with its structure, not with agents put onto its nodes. In this semi-directed Barabási-Albert model one can put in neighbour relations which are directed or undirected, for agents(spins) put onto the network nodes; but we do not that here.

Finally, for both SDBA1 and SDBA2 networks we found a Vogel-Fulcher law, suggesting stable ferromagnetism for T < Tc(N). For Potts model with q = 3 on SDBA1 and SDBA2 networks we found a tunneling between these three states with the evolution of time. Similarly, to the Ising model on undirected Barabási-Albert network there is no usual ferromagnetic transition on these SDBA1 and SDBA2 networks, since Tc(N) increases roughly logarithmically with network size N. The distribution of the number of neighbours of each node decays with a non-universal exponent depending on m.

It was known already that in the SDBA the $\boldsymbol{n(K)} \approx \boldsymbol{1/k^2}$ in opposition to $\boldsymbol{1/k^3}$ for standard BA networks at all m. Now we found for both SDBA1 and SDBA2 the variation with network size N size for large m and also showed the gap in the $\boldsymbol{K(i)}$ distribution at i = m for both types of networks.

Sources and References

1. Adamic, L. A., & Huberman, B. A. (2000). Power-law distribution of the world wide web. *Science, 287*(5461), 2115-2115.
2. Albert, R., & Barabási, A.-L. (2002). Statistical mechanics of complex networks. *Reviews of modern physics, 74*(1), 47.
3. Aleksiejuk, A., Hołyst, J. A., & Stauffer, D. (2002). Ferromagnetic phase transition in Barabási–Albert networks. *Physica A: Statistical Mechanics and its Applications, 310*(1), 260-266.
4. Arrhenius, S. (1889). Über die Reaktionsgeschwindigkeit bei der Inversion von Rohrzucker durch Säuren. *Zeitschrift für physikalische Chemie, 4*, 226-248.
5. Ashkin, J., & Teller, E. (1943). Statistics of two-dimensional lattices with four components. *Physical Review, 64*(5-6), 178.
6. Barabási, A.-L., & Albert, R. (1999). Emergence of scaling in random networks. *Science, 286*(5439), 509-512.
7. Barabási, A.-L., Albert, R., & Jeong, H. (2000). Scale-free characteristics of random networks: the topology of the world-wide web. *Physica A: Statistical Mechanics and its Applications, 281*(1), 69-77.
8. Barabási, A.-L., & Frangos, J. (2014). *Linked: the new science of networks science of networks*: Basic Books.
9. Beaudin, L., Ellis-Monaghan, J., Pangborn, G., & Shrock, R. (2010). A little statistical mechanics for the graph theorist. *Discrete Mathematics, 310*(13), 2037-2053.
10. Bertini, E., Kennedy, J., & Puppo, E. Interaction with uncertainty in visualisations.
11. Chang, S.-C., & Shrock, R. (2001). Exact partition function for the Potts model with next-nearest neighbor couplings on arbitrary-length ladders. *International Journal of Modern Physics B, 15*(05), 443-478.
12. Choudhury, A. R., Malhotra, A., Bhattacharjee, P., & Prasad, G. (2014). Facile and rapid thermo-regulated biomineralization of gold by pullulan and study of its thermodynamic parameters. *Carbohydrate polymers, 106*, 154-159.
13. Curie-point. Retrieved from http://www.britannica.com/EBchecked/topic/146902/Curie-point
14. Fitzpatrick, R. (2006). Classical Electromagnetism: An intermediate level course. *The University of Texas at Austin*, U.S.A.
15. Gibrat, R., & Les Inégalites Économiques, L. d. R. (1931). Sirey. *Paris, France*.
16. Guimarães Jr, P. R., de Aguiar, M. A., Bascompte, J., Jordano, P., & Dos Reis, S. F. (2005). Random initial condition in small Barabasi-Albert networks and deviations from the scale-free behavior. *Physical Review E, 71*(3), 037101.
17. Heise, D., Heß, M., Strecker, S., & Frank, U. (2010). Rekonstruktion eines klinischen Behandlungspfads mithilfe domänenspezifischer Erweiterungen einer Geschäftsprozessmodellierungssprache: Anwendungsfall und Sprachkonzepte *Dienstleistungsmodellierung 2010* (pp. 210-227): Springer.
18. Hong, P., Damrauer, N. H., Carroll, P. J., & Berry, D. H. (1993). Reaction chemistry of a tungsten disilene complex: net one atom insertion of chalcogens into Cp2W (. eta. 2-Me2Si: SiMe2). *Organometallics, 12*(9), 3698-3704.

19. Huang, K. (2009). *Introduction to statistical physics*: CRC Press.
20. Iordache, D.-A. (2000). *Numerical physics Specific problems and applications Dan-Alexandru Iordache.* Paper presented at the Proceedings of The First French-Romanian Colloquium of Numerical Physics.
21. Jeong, H., Tombor, B., Albert, R., Oltvai, Z. N., & Barabási, A.-L. (2000). The large-scale organization of metabolic networks. *Nature, 407*(6804), 651-654.
22. Jiang, Y. (1996). Extended large-Q Potts model simulation of foam drainage. *Philosophical Magazine Letters, 74*(2), 119-128.
23. Kaltenbrunner, A., Gómez, V., Moghnieh, A., Meza, R., Blat, J., & López, V. (2007). Homogeneous temporal activity patterns in a large online communication space. *arXiv preprint arXiv:0708.1579*.
24. Kurinsky, N. (2015). Monte Carlo Simulation of the Potts Model in 2-5 Dimensions.
25. Lander, E. S., Linton, L. M., Birren, B., Nusbaum, C., Zody, M. C., Baldwin, J., . . . FitzHugh, W. (2001). Initial sequencing and analysis of the human genome. *Nature, 409*(6822), 860-921.
26. Lima, F. (2015). Evolution of egoism on semi-directed and undirected Barabási-Albert networks. *International Journal of Modern Physics C, 26*(12), 1550135.
27. M. A. Sumuor, F. W. S. L., M.A. Radwan, M. M. Shabat. (2015). Natural Sciences Series. . *Al-Aqsa University Journal*, 50, Gaza,Palestin
28. Merton, R. K. (1968). The Matthew effect in science. *Science, 159*(3810), 56-63.
29. Newman, M., Barabasi, A.-L., & Watts, D. J. (2006). *The structure and dynamics of networks*: Princeton University Press.
30. Partition function (statistical mechanics). Retrieved from http://www.astro.lu.se/Education/utb/ASTA21/pdf/Partition%20function%20(statistical%20mechanics).pdf
31. Peierls, R. (1936). *On Ising's model of ferromagnetism.* Paper presented at the Mathematical Proceedings of the Cambridge Philosophical Society.
32. Potts, R. B. (1952). *Some generalized order-disorder transformations.* Paper presented at the Mathematical proceedings of the cambridge philosophical society.
33. Price, D. d. S. (1976). A general theory of bibliometric and other cumulative advantage processes. *Journal of the American society for Information science, 27*(5), 292-306.
34. Radwan, M., Sumour, M. A., Elbitar, A., Shabat, M., & Lima, F. (2016). Finite-size effects on semi-directed Barabási–Albert networks. International Journal of Modern Physics C, 1650109.
35. Renn, J. (1997). Einstein's controversy with Drude and the origin of statistical mechanics: A new glimpse from the "Love Letters". *Archive for history of exact sciences, 51*(4), 315-354.
36. Sanyal, S., & Glazier, J. A. (2006). Viscous instabilities in flowing foams: A Cellular Potts Model approach. *Journal of Statistical Mechanics: Theory and Experiment, 2006*(10), P10008.
37. Schubert, J. (2008). Clustering decomposed belief functions using generalized weights of conflict. *International journal of approximate reasoning, 48*(2), 466-480.

38. Simon, H. A. (1960). Some further notes on a class of skew distribution functions. *Information and Control, 3*(1), 80-88.
39. Stauffer, D. (2015). Zufallsnetze und Small Worlds *Handbuch Modellbildung und Simulation in den Sozialwissenschaften* (pp. 579-594): Springer.
40. Sumour, M., Lima, F., Radwan, M., & Shabat, M. Distribution of number of neighbours on semi-directed Barab'asi-Albert networks with many initial neighbours.
41. Sumour, M., & Radwan, M. (2012). Nonuniversality In Semi-Directed Barabási–Albert Networks. *International Journal of Modern Physics C, 23*(09), 1250062.
42. Sumour, M. A., & Lima, F. (2014). EPJ Plus.
43. Sumour, M. A., & Shabat, M. (2005). Monte Carlo Simulation Of Ising Model On Directed Barabasi–Albert Network. *International Journal of Modern Physics C, 16*(04), 585-589.
44. Sumour, M. A., Shabat, M., & Stauffer, D. (2005). Absence of ferromagnetism in Ising model on directed Barabasi-Albert network. *arXiv preprint cond-mat/0504460*.
45. Sun, L., Chang, Y., & Cai, X. (2004). A discrete simulation of tumor growth concerning nutrient influence. *International Journal of Modern Physics B, 18*(17n19), 2651-2657.
46. Swendsen, R. H., & Wang, J.-S. (1987). Nonuniversal critical dynamics in Monte Carlo simulations. *Phy. Rev. lett., 58*(2), 86.
47. Tran, H. (2013). q-State Potts model - Theory and simulation
48. Venter, J. C., Adams, M. D., Myers, E. W., Li, P. W., Mural, R. J., Sutton, G. G., . . . Holt, R. A. (2001). The sequence of the human genome. *Science, 291*(5507), 1304-1351.
49. Veselago, V., & Vinokurova, L. (1988). *The Magnetic and Electron Structures of Transition Metals and Alloys* (Vol. 3): Nova Publishers.
50. Wang, F., & Landau, D. (2001). Efficient, multiple-range random walk algorithm to calculate the density of states. *Phy. Rev. lett., 86*(10), 2050.
51. Wasserman, S., & Faust, K. (1994). *Social network analysis: Methods and applications* (Vol. 8): Cambridge university press.
52. Welsh, D. J., & Merino, C. (2000). The Potts model and the Tutte polynomial. *Journal of Mathematical Physics, 41*(3), 1127-1152.
53. Yule, G. U. (1925). A mathematical theory of evolution, based on the conclusions of Dr. JC Willis, FRS. *Philosophical Transactions of the Royal Society of London. Series B, Containing Papers of a Biological Character, 213*, 21-87.
54. Zhang, Y. L., Jiang, W., & Lin, L. (2014). *Composition-Property Relationships of Magnetic Inks for Screen Printing.* Paper presented at the Applied Mechanics and Materials.
55. Zipf, G. K. (1949). {Human Behaviour and the Principle of Least-Effort}.

Appendix

Appendix 1

Fortran program for Ising model on SDBA1, without spins.

```
      parameter(nrun=100,  maxtime=1000000,m=64,iseed=2,max=maxtime+m,
     1   kb=9000000,length=1+(1+m)*maxtime+m*(m-1))
      integer*8  ibm
      real*8  factor
      dimension  nklog(0:30)
      dimension  k(max),  nk(kb),  list(length)
      data  nk/kb*0/,nklog/31*0/
      OPEN  (UNIT=60,FILE='SDBA1-1NmA64.DAT')
      OPEN  (UNIT=70,FILE='SDBA1-2mA64.DAT')
      WRITE  (60,*)'#(nrun,  maxtime,  m,  iseed)',nrun,  maxtime,  m,iseed
      ibm=2*iseed-1
      factor=(0.25d0/2147483648.0d0)/2147483648.0d0
      fac=1.0/0.69314
      do  5  irun=1,nrun
      do  3  i=1,m
      do  7  j=(i-1)*(m-1)+1,(i-1)*(m-1)+m-1
7     list(j)=i
3     k(i)=m-1
      L=m*(m-1)
      if(m.eq.1)  then
      L=1
      List(1)=1
      k(1)=1
      endif
C     All  m  initial  sites  are  connected  with  each  other
      do  1  n=m+1,max
      do  2  new=1,m
4     ibm=ibm*16807
      j=1.d0+(ibm*factor+0.5d0)*L
      if(j.le.0.or.j.gt.L)  goto  4
      j=list(j)
      list(L+new)=j
2     k(j)=k(j)+1
      L=L+m+1
      list(L)=  n
1     k(n)=1
      write(60,*),'#(irun)',  irun
      do  5  i=  1,max
5     nk(k(i))=nk(k(i))+1
      SUM=0
      do  6  i=1,m
      SUM=SUM+K(i)
6     write(60,*)  i,k(i)
      do  9  i=1,kb
      j=alog(float(i))*fac
9     nklog(j)=nklog(j)+nk(i)
      AVERGESUM=SUM/m
      jmax=(1.0 + alog(float(kb))*fac)
      do 10 j=0,jmax
      if(nklog(j).ne.0) write(70,*) sqrt(2.0)*2**j,nklog(j),j,AVERGESUM
10     if(nklog(j).ne.0) print*, sqrt(2.0)*2**j,nklog(j),j,AVERGESUM
      stop
      end
```

Appendix 2

Fortran program for Ising model on SDBA2, without spins.

```
      parameter(nrun=100, maxtime=1000000,m=64,iseed=2,max=maxtie+m,
     1          kb=9000000,length=1+(1+m)*maxtime+m*(m-1))
            integer*8 ibm
           real*8 factor
            dimension nklog(0:30)
            dimension k(max), nk(kb), list(length)
           data nk/kb*0/,nklog/31*0/,k/max*0/
              OPEN (UNIT=60,FILE='SDBA2-1M64.DAT')
              OPEN (UNIT=70,FILE='SDBA2-2M64.DAT')
            WRITE (60,*)'#(nrun, maxtime, m, iseed)',nrun, maxtime, m,iseed
           ibm=2*iseed-1
           factor=(0.25d0/2147483648.0d0)/2147483648.0d0
           fac=1.0/0.69314
              do 5 irun=1,nrun
              do 3 i=1,m
              do 7 j=(i-1)*(m-1)+1,(i-1)*(m-1)+m-1
     7       list(j)=i
     3        k(i)= m-1
              L= m*(m-1)
           if(m.eq.1) then
              L=1
            List(1)=1
             k(1)=1
           endif
     C       All m initial sites are connected with each other
               do 1 n=m+1,max
               do 2 new=1,m
     4        ibm=ibm*16807
              j=1.d0+(ibm*factor+0.5d0)*L
           if(j.le.0.or.j.gt.L) goto 4
            j=list(j)
             if(new.eq.1) k(j)=k(j)+1
           if(k(j).gt.kb .or. k(n).gt.kb) stop 9
             list(L+new)=j
     2         continue
                   L=L+m+1
            List(L)=n
     1          k(n)=m

            write(60,*) '# (irun )', irun
     do 5 i= m+1,max
     5        if(k(i).gt.m) nk(k(i)-m)=nk(k(i)-m)+1
     SUM=0
     do 6 i=1,m
     SUM=SUM+K(i)
     6        write(60,*) i,k(i)
```

```
        do 9 i=1,kb
        j=alog(float(i))*fac
9       nklog(j)=nklog(j)+nk(i)
        AVERGESUM=SUM/m
        jmax=(1.0 + alog(float(kb))*fac)
        do 10 j=0,jmax
    if(nklog(j).ne.0) write(70,*) sqrt(2.0)*2**j,nklog(j),j,AVERGESUM
10       if(nklog(j).ne.0) print*,sqrt(2.0)*2**j,nklog(j),j,AVERGESUM
        stop
        end
```

Appendix 3.

This is the Fortran program for Ising model on SDBA1and SDBA2. without spins.

```
parameter(kb=30000)
C   maxtime=sites
      parameter(nrun=100,maxtime=10000,m=3,iseed=1,max=maxtime+m,
1    length=1+(1+m)*maxtime+m*(m-1))
      integer*8 ibm,iex, summag,imag
       integer*4 mag
       real*8 factor,ex
      dimension is(max),iex(-kb:kb),neighb(max,kb)
       dimension k(max), nk(kb), list(length)
       data nk/kb*0/,nsteps/100000/,k/max*0/
       print *, max,m,nsteps,nsteps,iseed
       ibm=2*iseed-1
       factor=(0.25d0/2147483648.0d0)/2147483648.0d0
      do 9 itemp=100,1600,+100
        T = 0.01*itemp
       do 5 irun=1,nrun
        do 3 i=1,m
         do 7 j=(i-1)*(m-1)+1,(i-1)*(m-1)+m-1
7         list(j)=i
```

```
      jj=0
     do 71 j=1,m
    if(j.eq.i) goto 71
     jj=jj+1
     neighb(i,jj) = j
71    continue
3      k(i)=m-1
       L=m*(m-1)
      if(m.eq.1) then
       L=1
       List(1)=1
       k(1)=1
     neighb(1,1)=1
       endif
C     All m initial sites are connected with each other
      do 1 n=m+1,max
       do 2 new=1,m
4      ibm=ibm*16807
      j=1.d0+(ibm*factor+0.5d0)*L
     if(j.le.0.or.j.gt.L) goto 4
        j=list(j)
        k(n)=k(n)+1
       if(new.eq.1) k(j)=k(j)+1
       if(k(j).gt.kb) stop 9
        list(L+new)=j
c     n selects m sites j which will all influence n
c      n will influence only the first selected j
c      j is always added to LIST, n is added only once
c      k(i) is the number of sites neighb(i, . ) which will influence i
      neighb(n ,new)=j
```

```
      if(new.eq.1) neighb(j,k(j))=n
2     continue
      list(L+m+1)=n
       L=L+m+1
1       k(n)=m
       do 5 i=1,max
        k(i)=min0(k(i),kb)
5       nk(k(i))=nk(k(i))+1
C       ******************** ISING PART
         DO 20 I=1,MAX
20       IS(I)=1
        DO 21 IE=-KB,KB,1
        EX=EXP(-2*IE/T)
         IF(IE/T.LE.-20.0) EX= 1.0D9
         IF(IE/T.GE. 20.0) EX= 1.0D-9
21       IEX(IE)=2147483648.0D0*(4.0D0*EX/(1.0D0+EX)-2.0D0)*2147483648.0D0
         SUMMAG=0
        DO 22 MC=1,NSTEPS
         DO 23 I=1,MAX
          IE=0
        DO 24 NB=1,K(i)
24       IE=IE+IS(NEIGHB(I,NB))
         IE=IS(I)*IE
         IBM=IBM*16807
         IF(IBM.LT.IEX(IE)) IS(I)=-IS(I)
23       CONTINUE
          MAG =0
        DO 25 I=1,MAX
25       MAG=MAG+IS(i)
         IMAG=IABS(MAG)
```

```
22          IF(MC.GT.(NSTEPS/2)) SUMMAG=SUMMAG+IMAG
           AVERGESUMMAG=SUMMAG*2.0/(MAX*NSTEPS)
C           End of Ising part
9           PRINT *,T,AVERGESUMMAG
STOP
END
```

Appendix 4

single spin-flip Glauber dynamics with a probability $\boldsymbol{P}$

Metropolis (1953) detailed balance ensures convergence to equilibrium.

$$\boldsymbol{P(S_i)P(S_i \rightarrow S_j) = P(S_j)P(S_j \rightarrow S_i)}$$

in other words: $\frac{\boldsymbol{P(S_i \rightarrow S_j)}}{\boldsymbol{P(S_j \rightarrow S_i)}} = \frac{\boldsymbol{P(S_j)}}{\boldsymbol{P(S_i)}} = \boldsymbol{e^{-(E_j - E_i)/KT}}$

(Where the last equality follows from the Boltzmann probability).

Glauber dynamics:

$$\boldsymbol{P(S_i \rightarrow S_j) = e^{-(E_j)/KT} / (e^{-(E_j)/KT} + e^{-(E_i)/KT}}$$

$$= \frac{\mathbf{1}}{\left(\mathbf{1} + \boldsymbol{e^{\Delta(E_{ji})/KT}}\right)}$$

(Raissa D'Souza, Simulating Glauber dynamics for the Ising model)